Asia Pacific Research Initiative for Sustainable Energy Systems 2019 (APRISES19)

Office of Naval Research
Grant Award Number N00014-20-1-2270

Ocean Thermal Energy Conversion (OTEC) Heat Exchanger Development (June 2023 to January 2024)

Task 6

Prepared for
Hawai‘i Natural Energy Institute

Prepared by
Makai Ocean Engineering

February 2024

HNEI
Hawai‘i Natural Energy Institute
University of Hawai‘i at Mānoa

MAKAI OCEAN ENGINEERING

ANNUAL REPORT

Prepared For

HAWAII NATURAL ENERGY INSTITUTE

1680 East West Road, POST 109

Honolulu, HI, 96822

USA

Prepared By

MAKAI OCEAN ENGINEERING

PO Box 1206, Kailua, Hawaii 96734

February 8, 2024

TABLE OF CONTENTS

LIST OF FIGURES

LIST OF TABLES

1. INTRODUCTION

Makai Ocean Engineering has been developing Thin Foil Heat Exchangers (TFHX) for use in seawater-refrigerant, air-water, and water-water applications. This report summarizes work performed between June 2023 – January 2024.

In this period, Makai's efforts included improving TFHX fabrication methods; continued characterization of TFHX thermal and structural/mechanical performance, and investigation of biofouling mitigation methods.

TFHX Design Development

Makai introduced a new cassette design for large-scale (> 2 $MW_{thermal}$) heat exchangers that require large stacks of plates. The cassette design is expected to reduce the total unit cost by eliminating individual modules and improve performance by eliminating two 90° turns in the seawater path.

Makai also delivered an air cooling unit (TFAC) to Blue Ocean Mariculture (BOM) and will be tracking performance once BOM installs it.

TFHX Fabrication

Makai continued to improve the fabrication fixtures, parameters, and quality control capabilities to reduce the fabrication time while improving plate success rates.

TFHX Characterization

Makai's characterization efforts were focused on better understanding the parameters that affect fatigue life. In addition to the pattern design, Makai also evaluated the impact of process parameters such as the expansion pressure and incorporation of an extra unsupported expansion step on fatigue life.

TFHX Performance Testing

Makai fabricated four TFHXs for seawater-ammonia testing. Three of the four heat exchangers have been tested, each as an evaporator and a condenser. One heat exchanger remains to be tested.

Biofouling

Makai tested an automated in situ cleaning prototype. A baseline test for wider plate spacings was also initiated.

2. TFHX DESIGN DEVELOPMENT

In this period, Makai's TFHX design efforts focused on new 4-port pattern designs, cost-effective designs for large heat exchangers (including seawater spacer improvements), and finalizing the Thin-Foil Air Conditioning (TFAC) unit. Makai also conducted initial studies on another high temperature material, Haynes 282.

2.1. CASSETTE DESIGN FOR LARGE-SCALE TFHXS

Makai previously developed a modular, four-port design for applications which used plate-frame style heat exchangers. However, some limitations of existing plate-frame heat exchangers were also present in the four-port modular design: 1) increased external fluid pressure drop associated with two 90° turns, 2) module housings added substantial cost for large plate stacks, and 3) lack of access to clean the plates (manually or in situ). Makai developed a cassette-style housing for applications in which the limitations of the four-port design can be an obstacle to adoption of the TFHX.

Under separate funding, Makai has procured the components, started plate fabrication, and will be testing the new cassette design at the 2-$MW_{thermal}$ scale.

2.2. THIN-FOIL AIR CONDITIONER (TFAC)

Blue Ocean Mariculture (BOM) expressed interest in Makai's Thin-Foil Air Conditioning (TFAC) unit which uses an off-the-shelf box fan and cold seawater to provide cooling and dehumidification for environmental control (Figure 1). Currently BOM is using diesel generators to power split A/C units for cooling.

In previous iterations of the TFAC, Makai identified flaws on components that resulted in poor seals between the plates. In this period, the flaws were corrected and Makai constructed and pressure-tested a TFAC unit. This unit was delivered to BOM and Makai awaits their installation and feedback on performance.

Figure 1. Assembled TFAC unit with nameplate for Blue Ocean Mariculture.

2.3. FULL-LENGTH, MODULAR, FOUR-PORT TFHX

Makai continues to fabricate and performance test (at the 100-kW scale) the four-port modular TFHX. In this period, Makai constructed 4 design variations (Table 1). Performance testing results are discussed separately in Section 4.

Table 1. Overview of full-length configurations constructed to date.

		# Plates	Plate Spacing [mm]	Foil Thickness ["]	Internal Channel Size [mm]	External Channel Size [mm]	HX Area [m2]
Previous	**TFHX-FL1**	24	2.12	0.005	0.589	1.275	10.32
	TFHX-FL2	24	2.12	0.005	0.9	0.964	10.32
	TFHX-FL3	12	4.24	0.005	0.9	0.964	5.16
	TFHX-FL4	24	2.12	0.005	0.78	1.084	10.32
	TFHX-FL5	12	2.12	0.005	0.78	1.084	5.16
	TFHX-FL6	6	4.24	0.005	0.78	3.202	2.58
	TFHX-FL7	12	2.12	0.005	0.503*	1.362*	5.16
	TFHX-FL8	6	4.24	0.005	0.562	3.421	2.58
	TFHX-FL9	12	2.12	0.005	0.560*	1.304*	5.16
	TFHX-FL10	12	2.12	0.005	0.838	1.026	5.16
New this Period	**TFHX-FL11**	12	2.12	0.005	0.737	1.129	5.16
	TFHX-FL12	12	2.12	0.005	0.636	1.228	5.16
	TFHX-FL13	12	2.12	0.005	0.736	1.128	5.16
	TFHX-FL14	12	2.12	0.005	0.579	1.285	5.16

2.4. PLATE SPACING

TFHX performance is dependent on accurate plate spacing so external flow is evenly distributed.

2.5. HIGH TEMPERATURE MATERIAL DEVELOPMENT

Makai has been investigating TFHX suitability for high temperature high pressure (HTHP) applications such as concentrated solar power (CSP). HTHP applications typically utilize expensive nickel-based alloys such as Inconel 625 or Haynes 230 which maintain their strength at temperatures > 650°C. Makai previously reported success in making a TFHX prototype plate out of 0.004” Haynes 230 that had a burst pressure > 3,000 psi at room temperature. In this period, Makai developed weld parameters, patterns, and tested two additional materials/thicknesses, 0.006” Haynes 230 and 0.006” Haynes 282.

Using 0.006” Haynes 230, Makai designed a prototype plate with 7,150 psig burst pressure and an effective channel size of 0.267 mm (using 6,000 psig expansion pressure). This design was created to meet the operating conditions of Gen3 CSP of 720°C and 3,000 psig. However, creep and creep fatigue may require additional changes in material selection, foil thickness, and/or plate design. Makai intends to stack 10 plates together and test the unit in an oven to validate the pressure capacity at HTHP.

Makai also experimented with 0.006” Haynes 282, a material that has a lower percentage of temperature-related reduction in strength at temperatures > 650°C and is reported to be more resistant to creep and creep fatigue. We were able to develop weld parameters to join two pieces of Haynes 282 together but the resulting plates had half the predicted burst pressure. After consulting with Haynes International, we learned a post-weld heat treatment is required for Haynes 282 to attain the cited strength. The post-weld heat treatment involves heating a sample to 1050-1135°C for 5 minutes and then reducing the temperature to 800°C and holding it for 4 hours. Development with Haynes 282 is currently on hold pending the results of testing with Haynes 230.

3. TFHX Fabrication

Makai continues to focus fabrication efforts on improving efficiency and success rates to achieve fast, reliable, repeatable, high-quality TFHX plates. This includes revisions to improve existing equipment and fixturing and tooling and methods to improve weld quality control and repair.

In this period, Makai focused on:

- Troubleshooting plate failures and identifying fixturing-related issues,
- New fixturing to improve cut edge quality,
- New fixturing and quality control methods to repair welds after expansion,
- Optimizing parameters to reduce plate fabrication time.

3.1. QUALITY CONTROL

Control of fabrication environment is one way to improve the weld success rate. A second method is to identify and repair defective welds, to produce an overall successful plate. Makai previously reported on using high-resolution imaging to autonomously identify and repair defective welds. However, some weld defects cannot be identified using imaging but are identified manually during leak checks. In this period, Makai developed a method and designed fixturing to perform repairs on weld defects identified during manual leak checks. This method adds 20% to fabrication time, which is faster than making a new plate and does not require additional raw materials. Makai will continue to improve this method.

3.2. LASER CUTTING STATION

Makai previously reported poor cut edge quality on finished plates that required an additional grinding step, particularly for dP-sensitive applications. In this period, a series of trials was conducted to identify the variables affecting the quality of the cut edge and new fixturing to improve the cut edge quality was designed and commissioned. With the new fixturing, the quality of the cut edge has improved substantially, however there are still some sections with rough finish. The final step to a uniform smooth edge can be accomplished with software modification.

3.3. FABRICATION CHALLENGES

Makai overcame some challenges with fixturing and subsystem components but continues to struggle with fabrication consistency. Upcoming work will focus on component level testing to determine if unknown variations in the weld environment are leading to inconsistencies or if fundamental changes in fixturing are required.

3.4. ECONOMIC ANALYSIS

Categories that contribute to TFHX cost include: materials/components, labor, heat exchanger components (e.g., modules, endplates, hardware), consumables, and overhead. Previously, Makai's focus was on reducing material costs to make the TFHX cost competitive. In this period, Makai’s focus has been on reducing the plate costs by improving plate success rates and reducing fabrication time.

4. TFHX PERFORMANCE TESTING

In this period, Makai built 4 stand-alone TFHX units with different internal/external channels and plate spacings (Table 2). Three units were tested in a counterflow configuration as a condenser and an evaporator (Figure 2). Delays in repair parts required to operate the 100-kW Test Station prevented testing of TFHX-FL14, which will be completed in the next work period.

Table 2. Overview of TFHX test units.

	# Plates	Plate Spacing [mm]	Foil Thickness ["]	Internal Channel Size [mm]	External Channel Size [mm]	Fluid Length [m]	HX Area [m2]
TFHX-FL11	12	2.12	0.005	0.737	1.129	0.86	5.16
TFHX-FL12	12	2.12	0.005	0.636	1.228	0.86	5.16
TFHX-FL13	12	2.12	0.005	0.736	1.128	0.86	5.16
TFHX-FL14	12	2.12	0.005	0.579	1.285	0.86	5.16

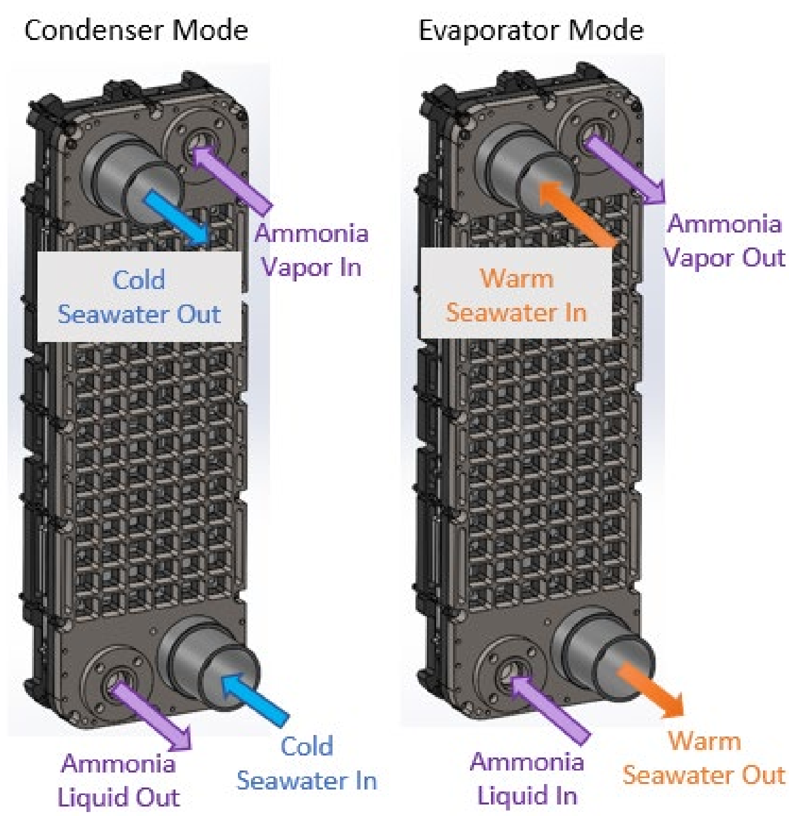

Figure 2. Full-length TFHX module configured for counterflow condenser and evaporator testing.

The pattern weld designs were specifically selected to have incremental changes in internal channel size (TFHX-FL11, -FL12, and -FL14) that can be compared with previous performance testing data. TFHX-FL13 was designed to have the same internal channel size as TFHX-FL11, but achieved with a different pattern weld spacing and expansion pressure. This should provide some insight on the relative importance of the effective channel height and aspect ratio.

TFHX-FL11 and -FL14 were constructed twice. In both heat exchangers, the seawater side pressure drop was observed to increase between the initial flow check and subsequent data collection points (Figure 3). After performance testing was completed (condenser and evaporator testing), disassembly revealed two plates had seal weld leaks that caused the area around the seawater manifold to inflate and block off a portion of the seawater flow area. Although only 2 plates had leaks, the inflated portion distorted the plate stack and obstructed part of the seawater entrance duct which explains the increase in measured seawater pressure drop. All new plates were fabricated and performance testing was repeated.

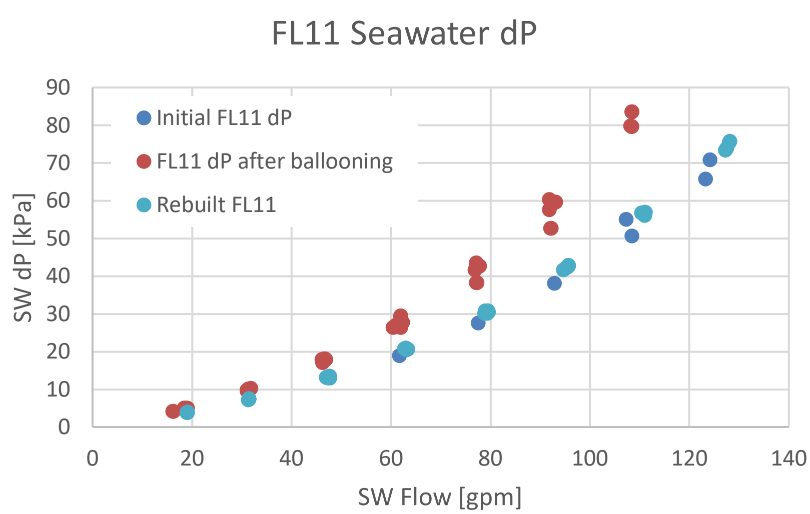

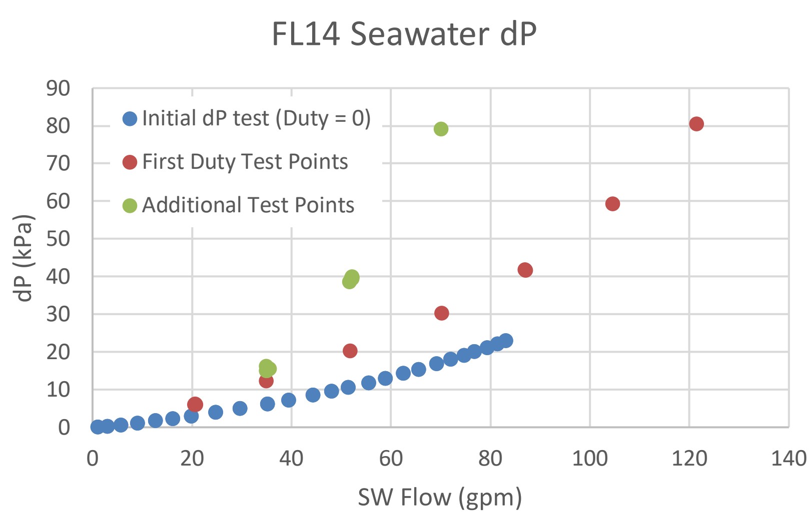

Figure 3. Substantial discrepancy in seawater pressure drop between initial and subsequent data points in FL11 and FL14. Upon disassembly, several plates had expanded areas between the internal and external seal welds which blocked off some of the seawater flow area.

4.1. 100-KW TEST STATION OPERATIONS

While testing FL14, a 4X increase in seawater pressure drop was observed between the initial flow test and later test points. Based on experience with FL11, seal weld leaks were suspected and testing was halted. FL14 was isolated from the system to prevent ammonia loss through the suspected leak. However, because FL14 was configured as a condenser, isolating FL14 resulted in a loss of cooling to the rest of the ammonia system which heated up due to ambient environmental conditions. In a saturated state, ammonia pressure increases with increasing ammonia temperature; to prevent over-pressurization, the 100-kW Test Station utilizes both vapor and liquid pressure relief valves. Vapor pressure relief valves are designed to provide quick pressure release if system pressure exceeds 250 psig. Liquid pressure relief valves are mainly intended as a safety measure in case a section of liquid piping is inadvertently isolated. In this situation, ammonia system conditions reached 35°C and 1250 kPa (abs) and a vapor pressure relief functioned to release pressure. However, subsequent pressure cycling (due to diurnal changes in ambient temperature) triggered a liquid relief valve to release early at ~1180 kPa abs. The valve also failed to fully reseat so liquid ammonia continued to release into the enclosure. Makai was alerted of the situation by neighbor tenants and immediately worked to secure the system.

To prevent future occurrences, Makai has set a maintenance cycle to replace relief valves. Makai suspects the location of malfunctioning relief valve (after the feed pump) may have contributed to its failure. The valve is subject to frequent vibration and changing pressurization between performance test points. Makai's new policy is to replace the relief valve after every 4th heat exchanger test to account for accelerated wear. Additional triggers have also been added to the automated emergency text alert system so Makai can be warned if conditions appear to be leading to a pressure release without intervention.

The replacement valves were a long-lead item and did not arrive in time for the 100-kW station to be recommissioned prior to the end of this work period. This task will be accomplished in the next work period along with FL14 performance testing.

Upon disassembly, 10 out of 12 FL14 plates had seal weld leaks. The seal weld leaks are consistent with the previously reported issue of contact between the plate and welding fixture during welding. 12 new FL14 plates were remade in preparation for performance testing.

4.2. SEAWATER-AMMONIA PERFORMANCE TESTING

TFHX-FL11, -FL12, and -FL13 were tested in condenser and evaporator configurations at energy densities between 5-20 kW/m^2 and seawater velocities between 0.3-1.8 m/s. Ammonia duty was controlled by controlling the seawater flow rate through the companion (APV) heat exchanger. For example, during evaporator testing, the APV heat exchanger functions as a condenser; increasing the cold seawater flow through the APV increases TFHX duty at a fixed TFHX seawater flow rate. Seawater flow was controlled by adjusting seawater control valves. During evaporator testing, the quality is set by adjusting the ammonia liquid flow rate using a VFD to control the feed pump.

4.2.1. Seawater Pressure Drop

Seawater-side pressure drop is related to the pumping power required to provide a certain seawater flow rate through the heat exchanger. The seawater pressure drop is mainly dependent on channel size and seawater velocity (Figure 4). At the same velocity, the pressure drop when tested as an evaporator versus a condenser should be comparable. Some plate designs exhibit limited expansion/contraction of the internal channel size with differences in internal vs external pressure and small deviations in pressure drop between evaporator and condenser mode are expected.

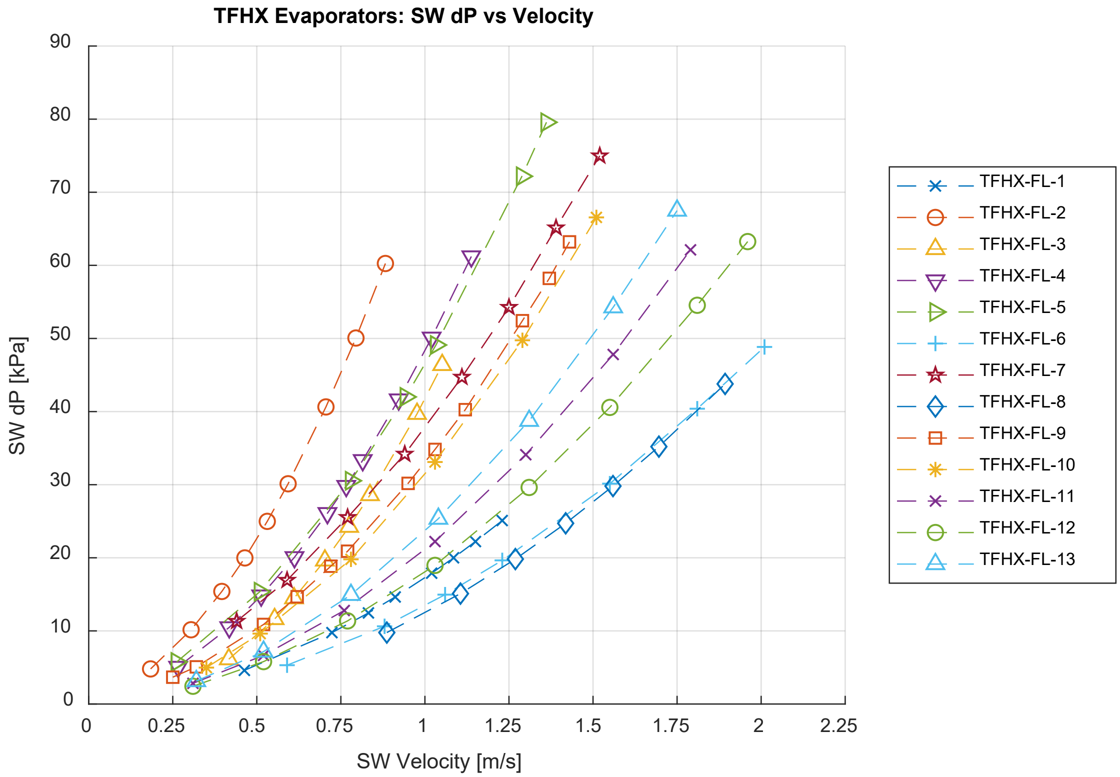

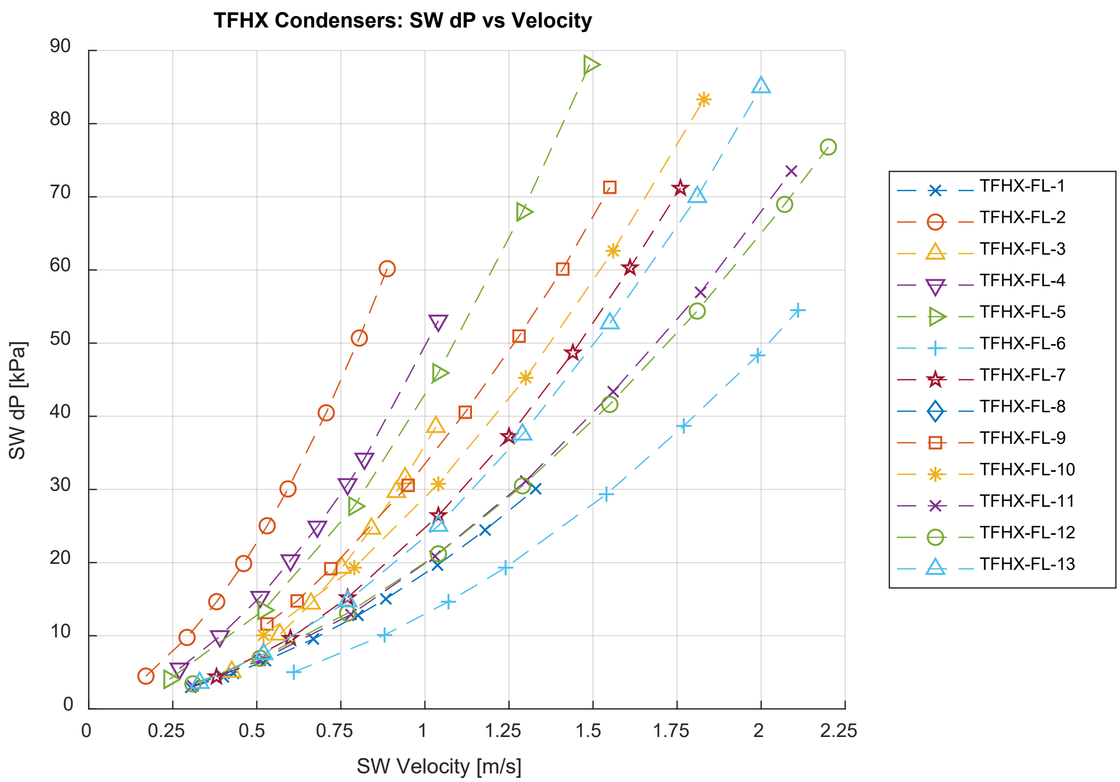

Figure 4. Seawater pressure drop for all tested TFHX units.

4.2.2. Ammonia Pressure Drop

Ammonia-side pressure drop is an important consideration for an evaporator/condenser. In a closed-cycle OTEC system, minimizing the pressure drop increases the available differential pressure across a turbine and reduces the pumping power required to recirculate refrigerant. Ammonia pressure drop is strongly dependent on ammonia vapor flow rate, quality, and heat exchanger geometry.

Ammonia-side pressure drop versus energy is shown for all 12-plate TFHX units plus TFHX-FL1 (24 plates) to minimize the effect of manifold duct losses and focus on the effect of internal channel size and pattern weld design (Figure 5). TFHX-FL1 is included because it has the smallest effective internal channel size. TFHX-FL1, -FL12, -FL13, -FL11, and -FL10 used the same weld diameter at different weld spacings to produce effective internal channels from 0.59 mm to 0.84 mm. TFHX-FL13 and -FL11 had the same effective internal channel size but used a different weld spacing and expansion pressures. TFHX-FL3, -FL5, and -FL6 had the same weld diameter and weld spacing but different expansion pressures to produce effective internal channel heights of 0.90 mm and 0.78 mm.

In both evaporator and condenser configurations, designs with the largest effective internal channel heights had the lowest pressure drop at the same energy density. For the same effective internal channel height, TFHX-FL13 had a tighter weld spacing compared to TFHX-FL11 and slightly higher pressure drop.

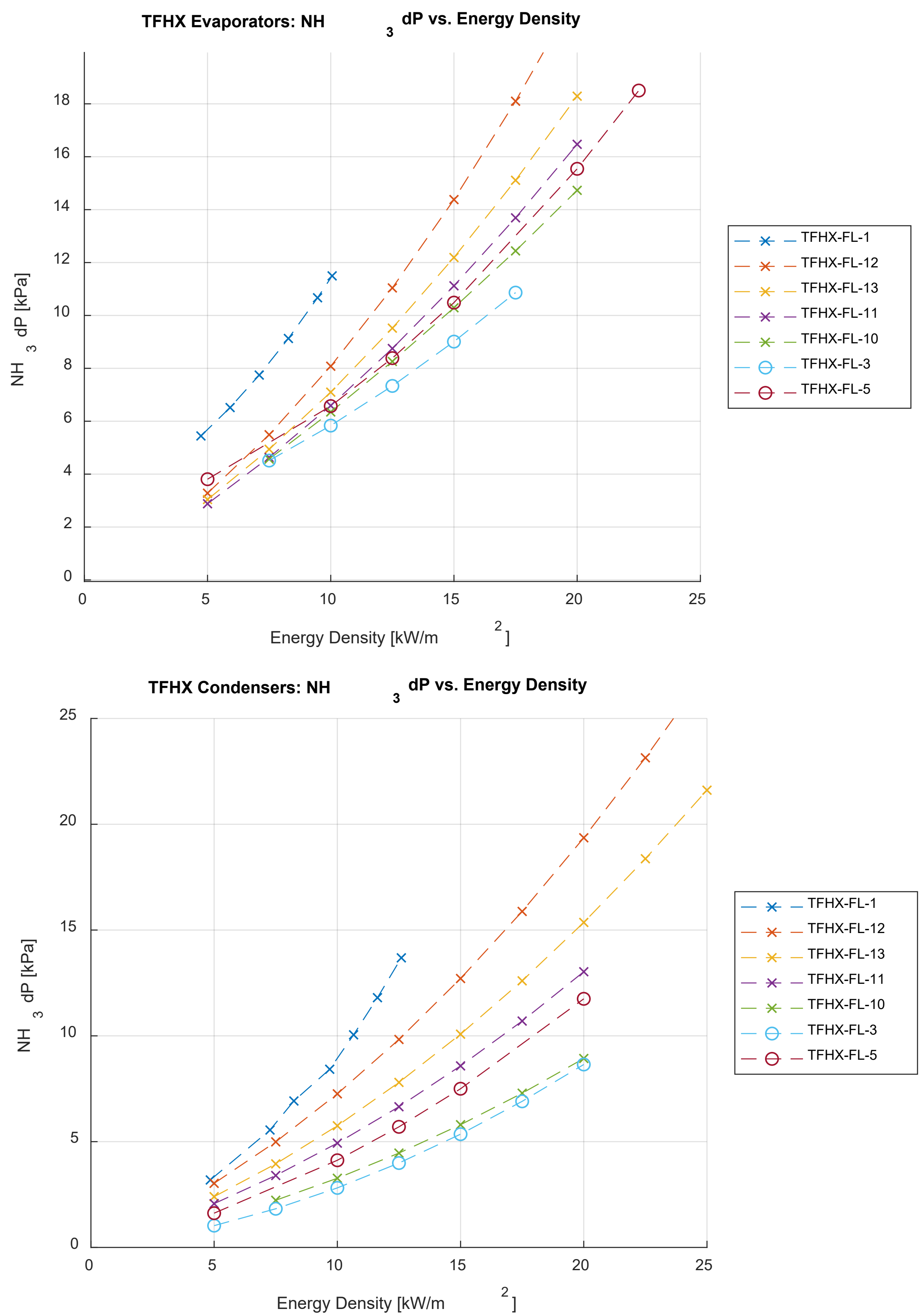

Figure 5. Ammonia pressure drop versus energy density for all 12-plate TFHX units.

4.2.3. <u>Overall Heat Transfer Coefficient</u>

U-value is predominantly dependent on seawater flow rate but duty (and quality for an evaporator) also has an effect. In both condenser and evaporator modes, U-value increases almost linearly with increasing seawater flow (Figure 6) over the range of the tested velocities. As an evaporator, at higher seawater velocities, a ~13% increase in U value is observed when increasing energy density from 5 kW/m^2 to 20 kW/m^2 (Figure 7). As a condenser, there is no significant difference in U value in the range of energy densities tested.

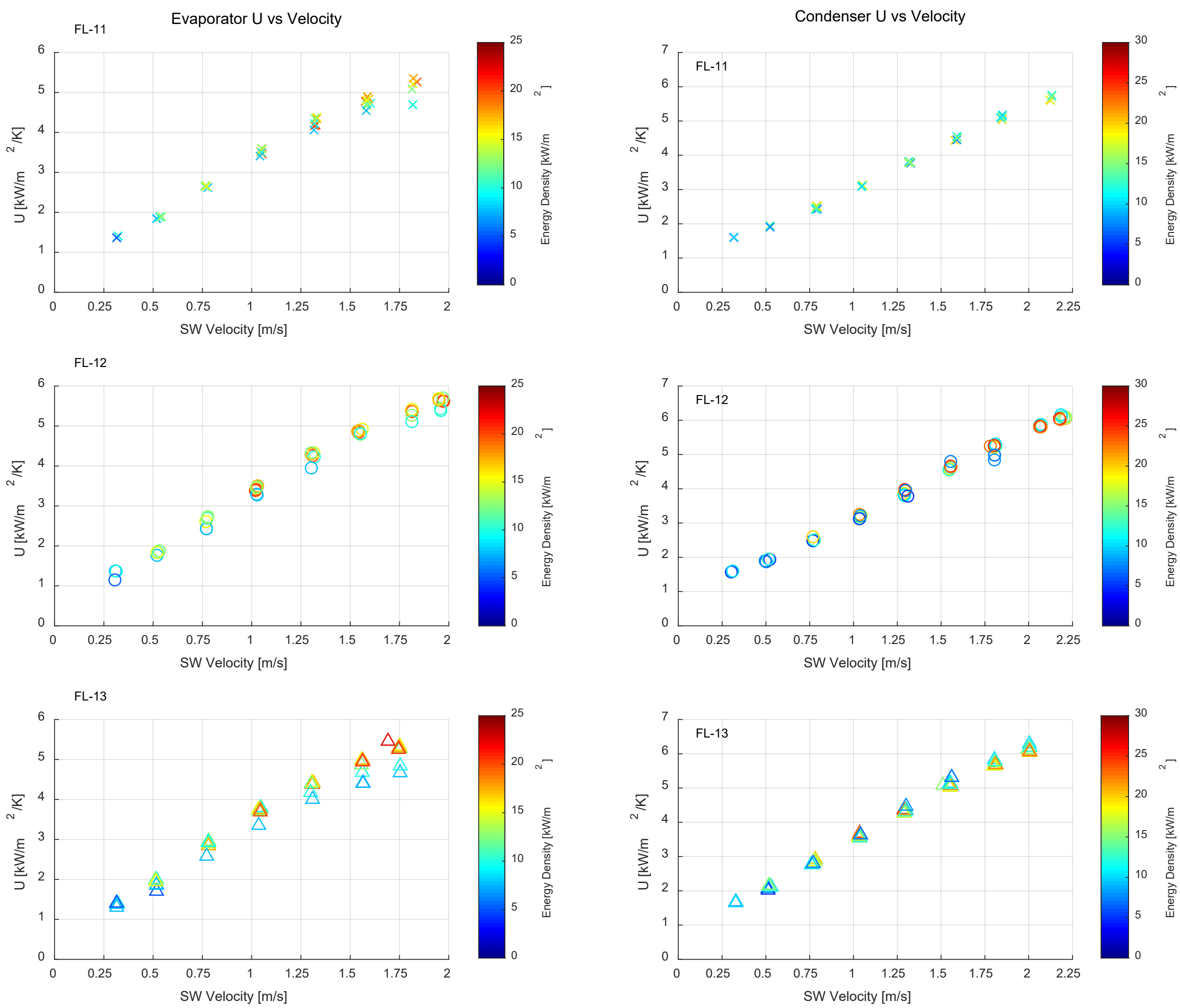

Figure 6. U-value vs seawater velocity.

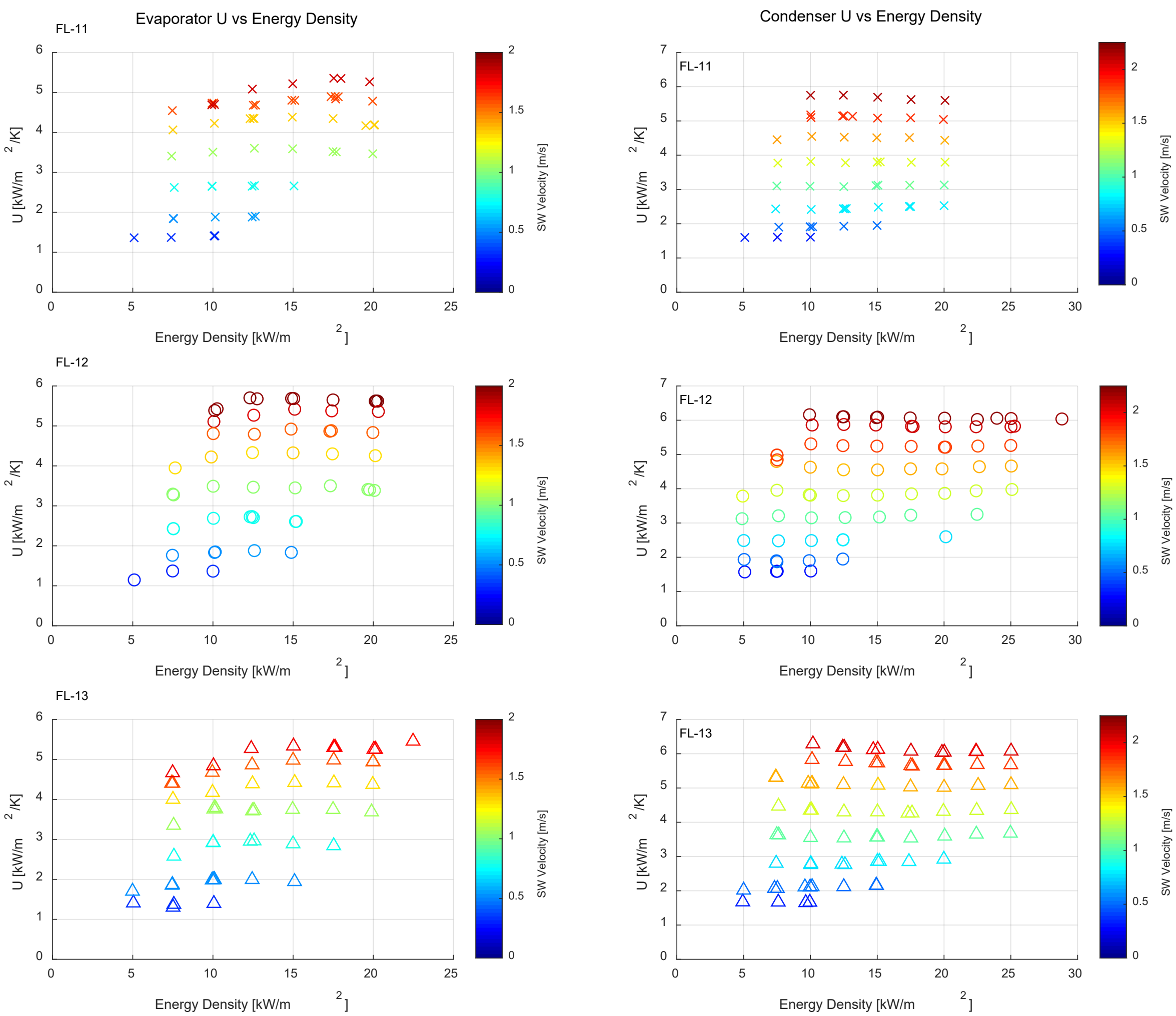

Figure 7. U-value vs energy density.

4.2.4. Convective Coefficients

Makai previously reported that there is substantial uncertainty surrounding convective coefficients due to mathematical limitations of solving equations where there are more unknowns than equations and the effects of averaged versus localized heat transfer performance.

Seawater Convective Coefficients

Seawater side convective coefficients were solved independently for each configuration (condenser or evaporator) for each TFHX unit. Except for FL-10, the external seawater convective coefficients between evaporator and condenser configurations are in agreement (Figure 8). Unlike previous results, seawater convective coefficients increase almost as a squared function with increasing seawater velocity.

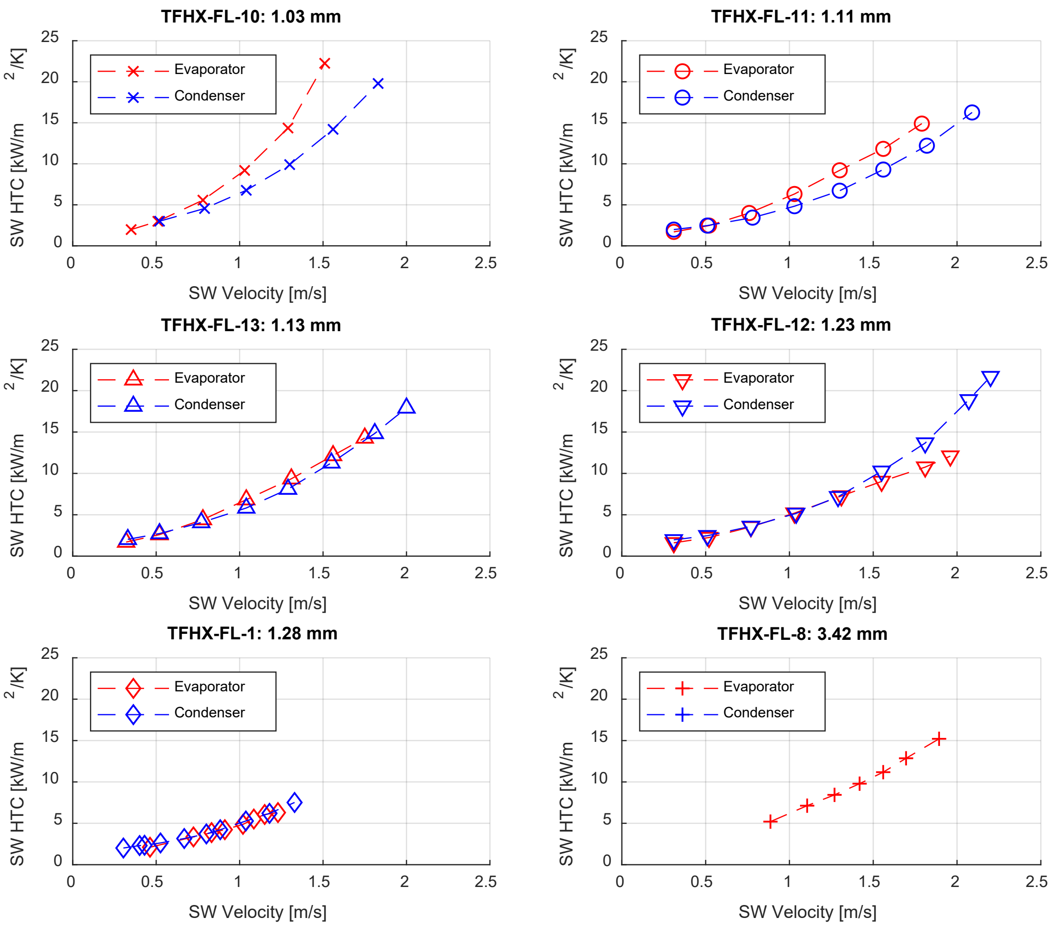

Figure 8. Seawater-side convective coefficients for TFHX units with different internal channel sizes and plate spacings. External channel size is shown after the unit number.

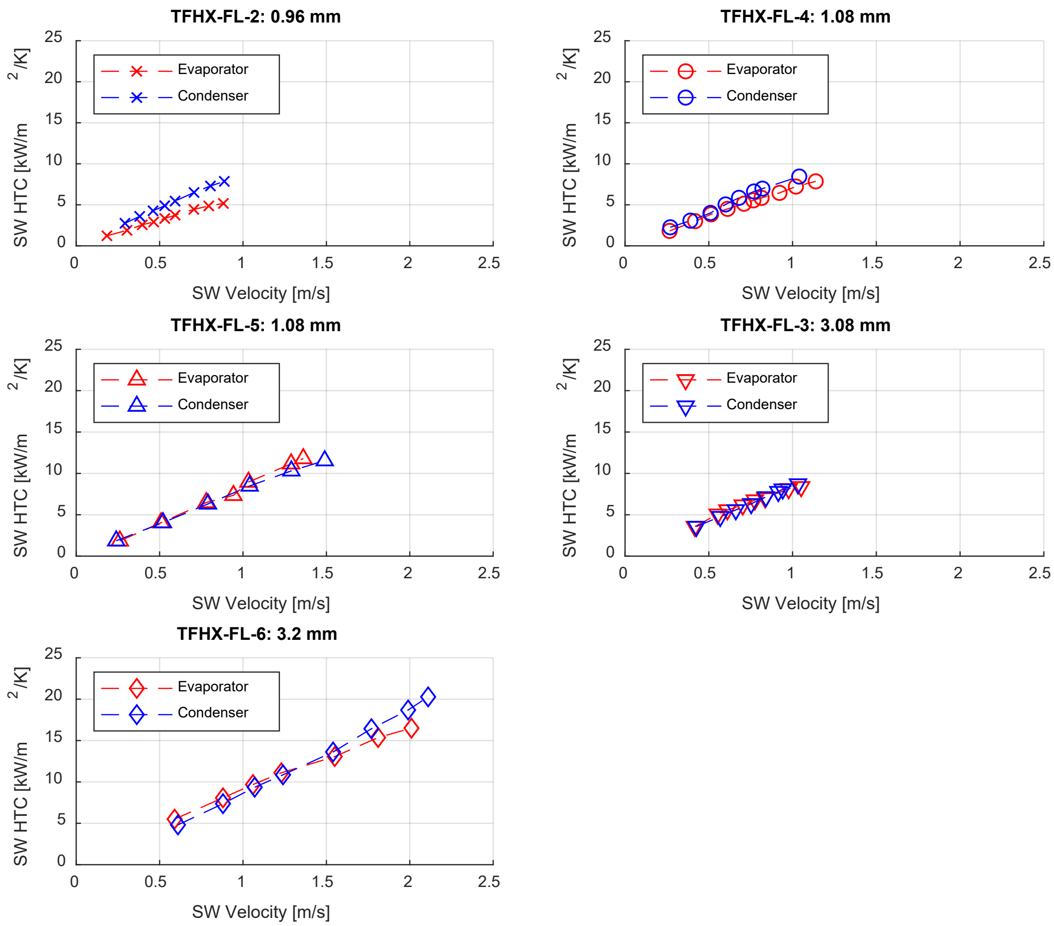

Figure 9. Seawater-side convective coefficients for TFHX units with the same weld design but different expansion pressures. External (seawater) channel size is shown after the unit number.

There is no clear trend between heat exchanger channel size and seawater convective coefficients (Figure 10). Heat exchangers with large seawater channels (FL-3 and FL-6) had among the highest seawater convective coefficients for the same velocity, but FL-8, which also had large seawater channels had lower seawater convective coefficients compared to heat exchangers with smaller seawater channels such as FL-5. Heat exchangers with comparable channel sizes had comparable convective coefficients at the same Reynolds number. For the same pressure drop, heat exchangers with larger channels had higher convective coefficients. For the same pumping power (represented by flow rate times pressure drop), there is no trend for convective coefficients and channel size. The smallest seawater channel (TFHX-FL2) had the lowest convective coefficient for the same pumping power. However, the largest channel sizes (TFHX-FL3 and -FL8) had the next lowest convective coefficients.

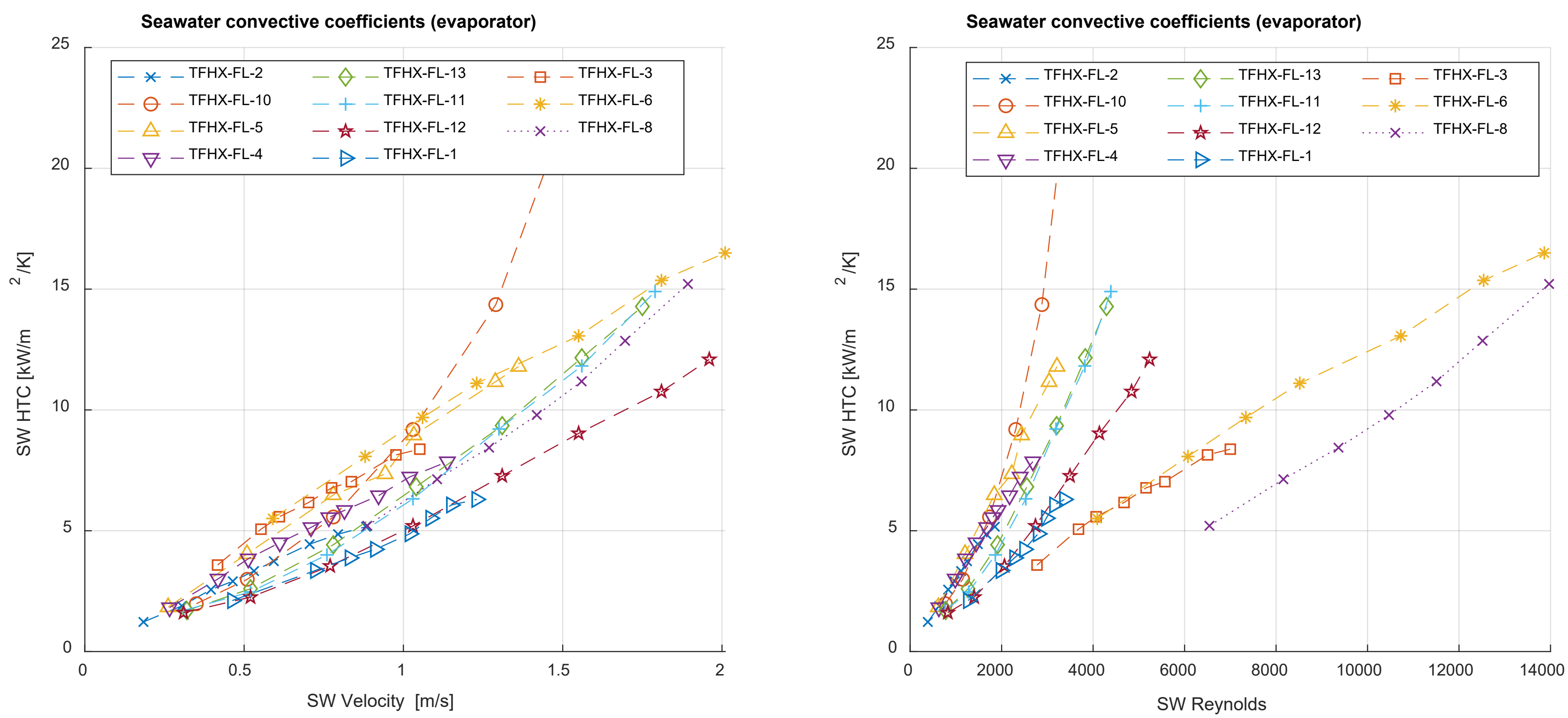
Seawater convective coefficients (evaporator)
TFHX-FL-2
TFHX-FL-10
TFHX-FL-5
TFHX-FL-4
TFHX-FL-13
TFHX-FL-11
TFHX-FL-12
TFHX-FL-1
TFHX-FL-3
TFHX-FL-6
TFHX-FL-8
SW HTC [kW/m^2/K]
SW Velocity [m/s]
Seawater convective coefficients (evaporator)
TFHX-FL-2
TFHX-FL-10
TFHX-FL-5
TFHX-FL-4
TFHX-FL-13
TFHX-FL-11
TFHX-FL-12
TFHX-FL-1
TFHX-FL-3
TFHX-FL-6
TFHX-FL-8
SW HTC [kW/m^2/K]
SW Reynolds

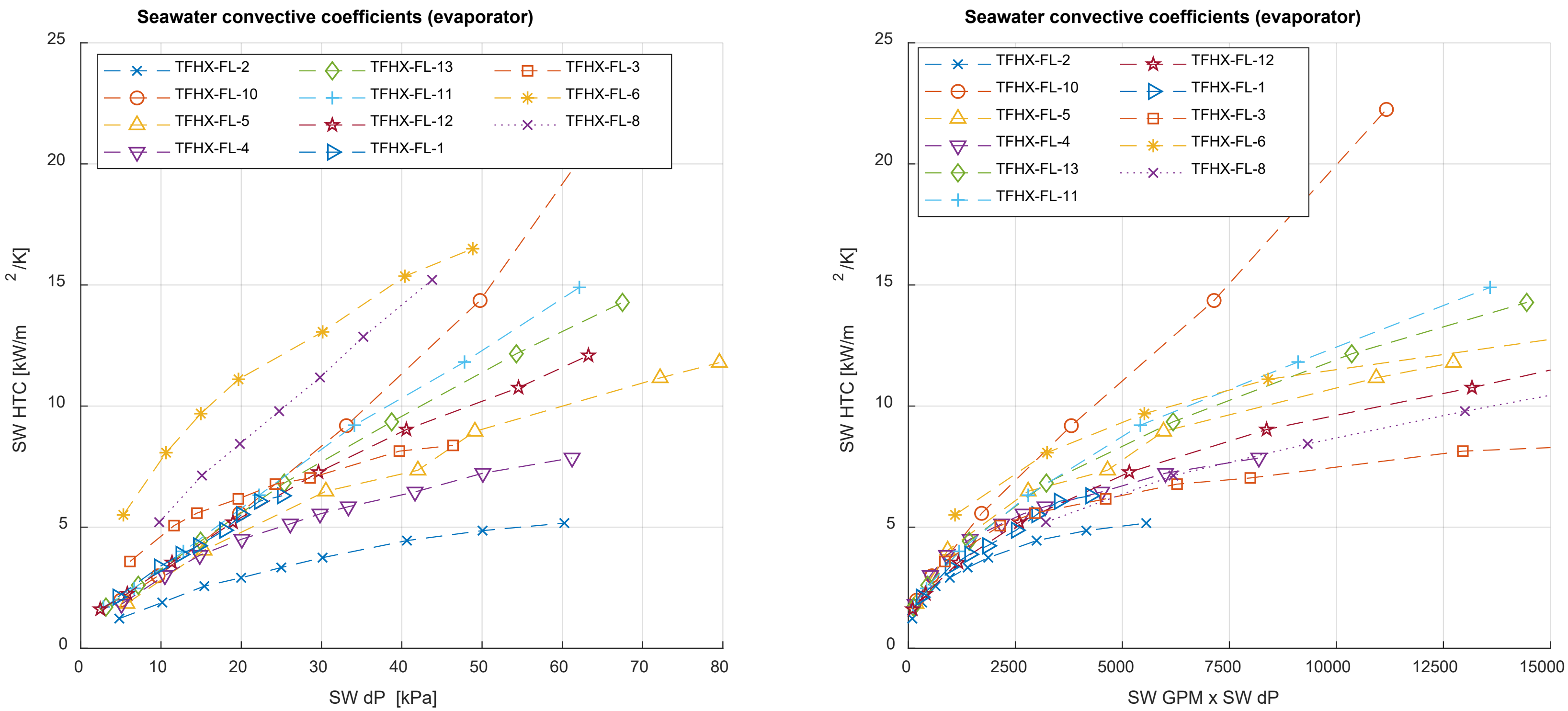

Figure 10. Evaporator seawater convective coefficients. TFHX units are listed from smallest seawater channel (TFHX-FL2) to largest (TFHX-FL8)

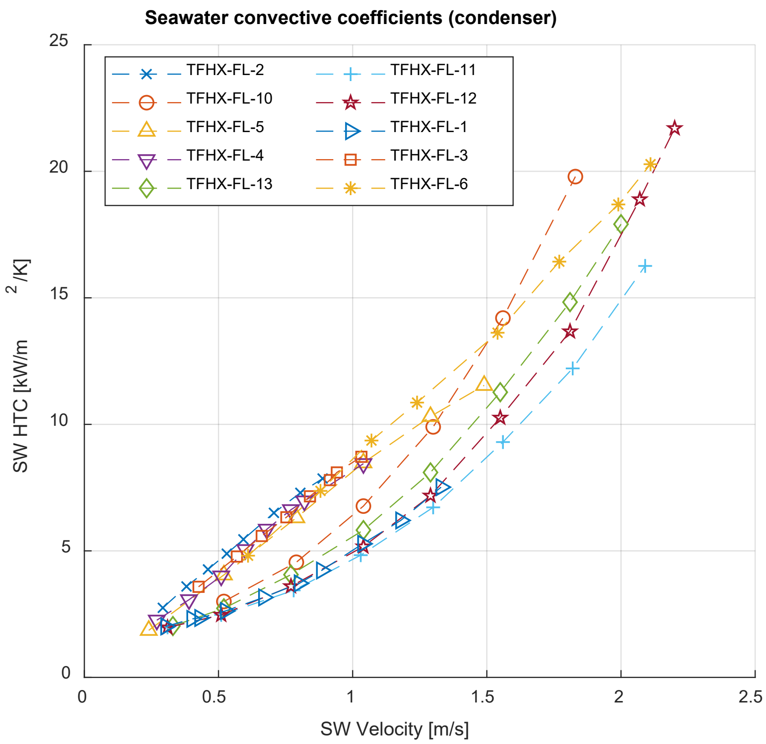
Seawater convective coefficients (condenser)
SW HTC [kW/m^2/K]
SW Velocity [m/s]
TFHX-FL-2
TFHX-FL-10
TFHX-FL-5
TFHX-FL-4
TFHX-FL-13
TFHX-FL-11
TFHX-FL-12
TFHX-FL-1
TFHX-FL-3
TFHX-FL-6

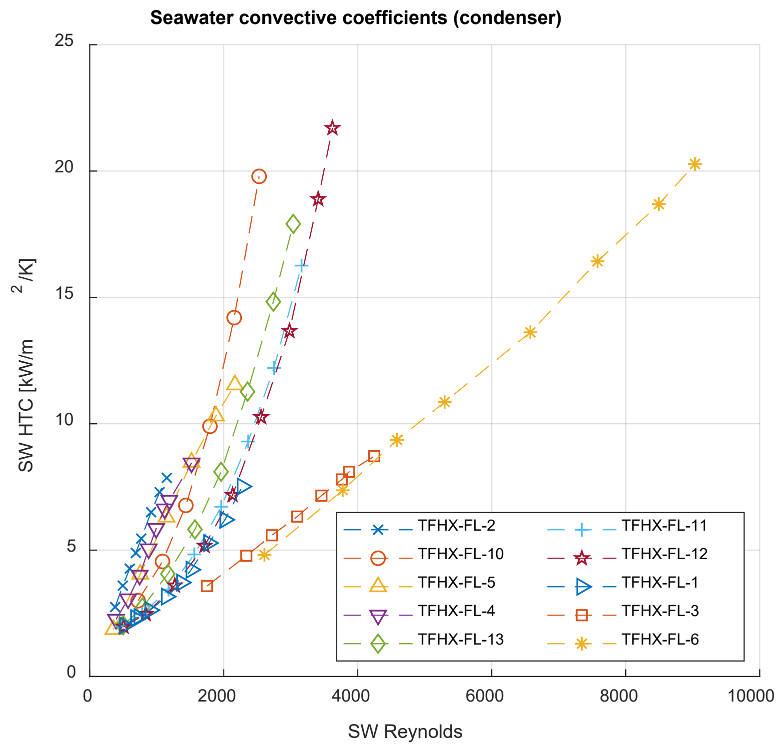
Seawater convective coefficients (condenser)
SW HTC [kW/m^2/K]
SW Reynolds
TFHX-FL-2
TFHX-FL-10
TFHX-FL-5
TFHX-FL-4
TFHX-FL-13
TFHX-FL-11
TFHX-FL-12
TFHX-FL-1
TFHX-FL-3
TFHX-FL-6

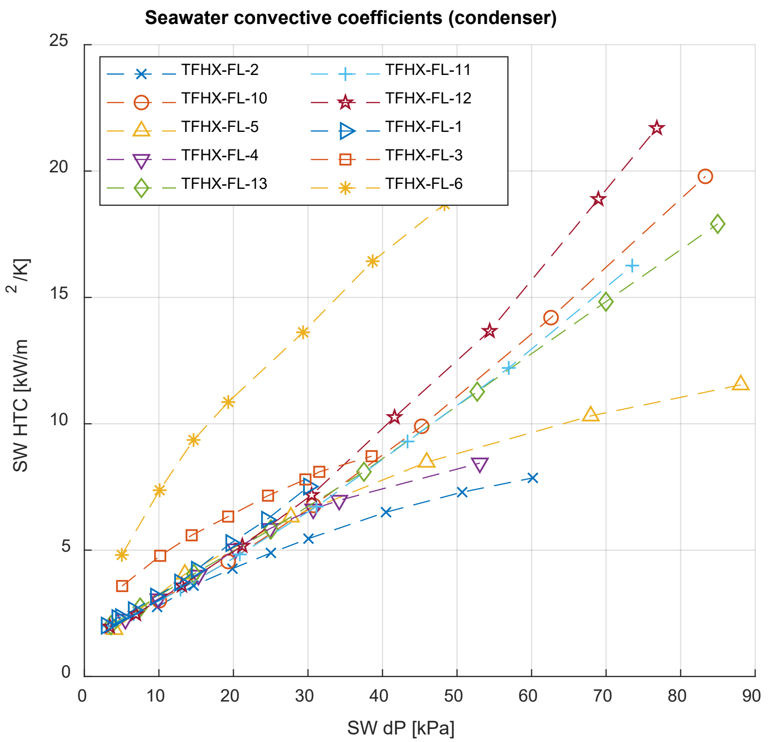

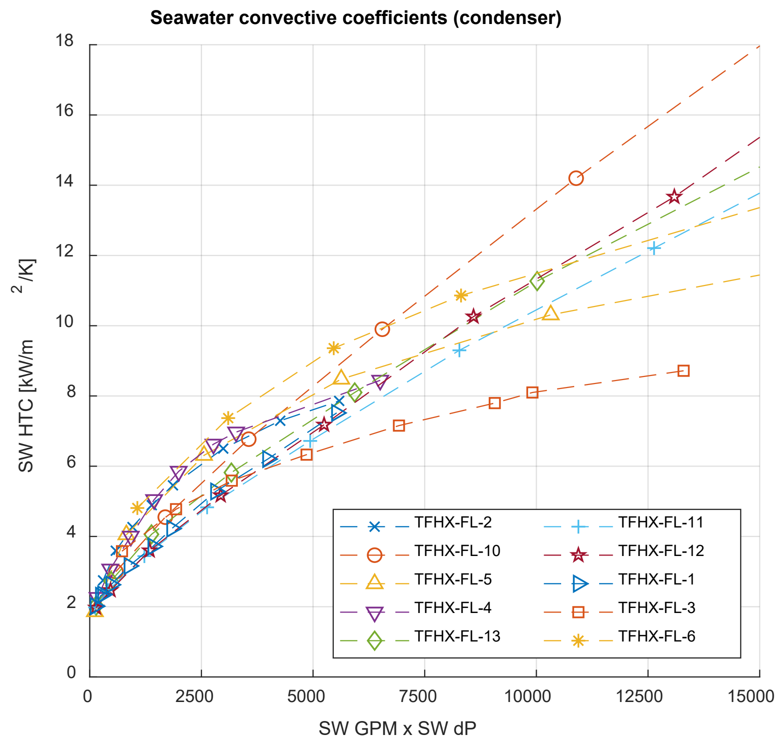

Figure 11. Condenser seawater convective coefficients. TFHX units are listed from smallest seawater channel (TFHX-FL2) to largest (TFHX-FL6)

Ammonia side convective coefficients.

Ammonia-side convective coefficients also did not have a clear trend with ammonia channel size (Figure 12). In general, ammonia convective coefficients increase with increasing energy density up to between 7.5 – 10 kW/m^2.

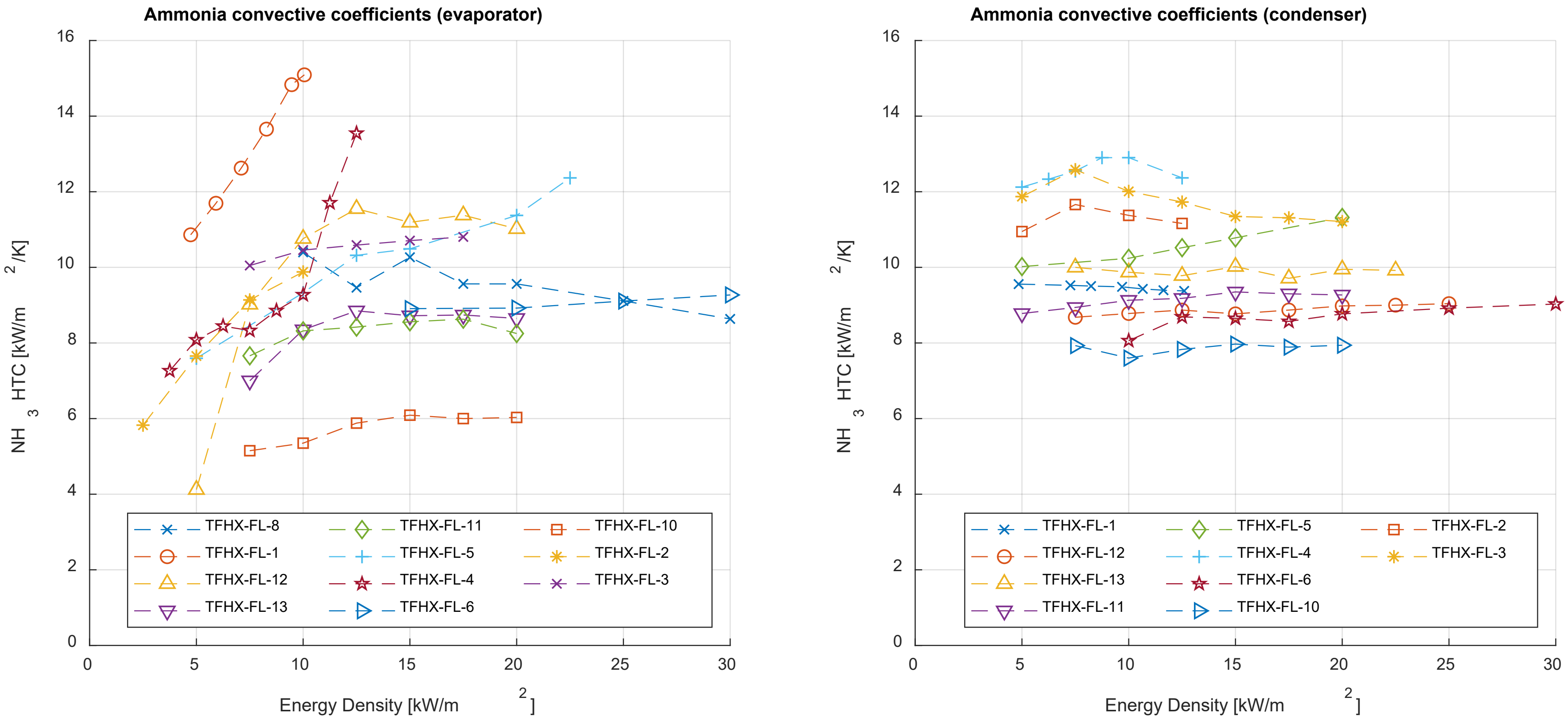

Figure 12. Ammonia-side convective coefficients for evaporator and condenser. TFHXs are listed from smallest ammonia effective channel (TFHX-FL8/-FL1) to largest (TFHX-FL3).

4.2.5. Heat Exchanger Approach Temperature

Heat exchanger approach temperature is determined by the seawater temperature, seawater flow rate, and duty. Makai is defining the approach temperature as:

$$T_{approach} = T_{warm\ seawater\ in} - T_{saturation\ at\ EOPS} \text{ (evaporator)}$$

$$T_{approach} = T_{saturation\ at\ CIPS} - T_{cold\ seawater\ in} \text{ (condenser)}$$

Makai's definition is customized for OTEC purposes; the ammonia saturation temperatures at the evaporator outlet and condenser inlet are used because these are directly connected to the turbine inlet/outlet. Additionally, because the bulk of the duty is in phase change, superheating at the condenser inlet is not accounted for and the saturation temperature is used instead of the measured temperature.

For OTEC operations, small approach temperatures result in higher available differential pressure across the turbine. Higher seawater flow rates yield smaller approach temperatures, but also require higher parasitic losses from high volumetric flow rates and/or high seawater pressure drops.

One way to compare heat exchanger performance is to match heat transfer areas and then compare the approach temperature versus pumping power at fixed energy densities (Figure 13 and Figure 14).

For both evaporator and condenser modes, TFHX units with 4.24-mm plate spacings (FL-3, FL-6, and FL-8) and, therefore, larger seawater channels, had the lowest approach temperatures for the same pumping power. FL-1 and FL-12 had the lowest approach temperatures of the TFHX units with 2.12-mm plate spacing and also had comparable approach temperatures compared to FL-3.

This analysis only considers the pumping power through the heat exchanger. For OTEC operations, the total volume of seawater flow is also important, particularly for the condenser. For example, although FL-3 and FL-6 had the lowest condenser approach temperatures, the both required up to 2.5X the flow as FL-4. Furthermore, at the same pumping power, FL-4 had 10% higher approach temperature than FL-1 but used 20% less volumetric flow. For a fixed cold water pipe size, lower volumetric flow rates have lower seawater system losses.

A comprehensive comparison of TFHX designs in the OTEC context will require a tradeoff study evaluating increase in net power production gained by smaller approach temperatures versus a larger cold water pipe and overall OTEC system (i.e., more expensive capital investment).

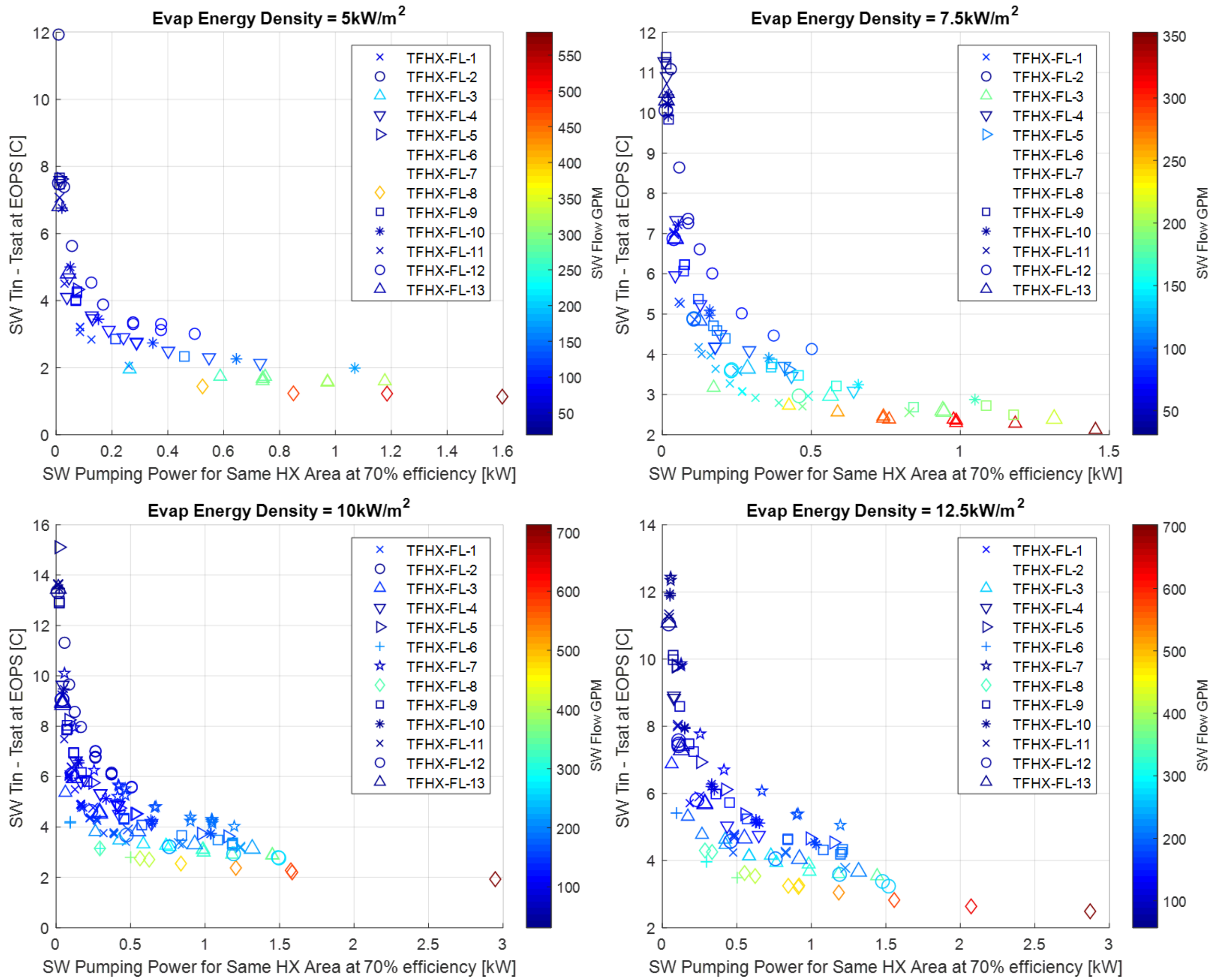

Evap Energy Density = 5kW/m2
SW Tin - Tsat at EOPS [C]
SW Pumping Power for Same HX Area at 70% efficiency [kW]
SW Flow GPM
TFHX-FL-1
TFHX-FL-2
TFHX-FL-3
TFHX-FL-4
TFHX-FL-5
TFHX-FL-6
TFHX-FL-7
TFHX-FL-8
TFHX-FL-9
TFHX-FL-10
TFHX-FL-11
TFHX-FL-12
TFHX-FL-13
Evap Energy Density = 7.5kW/m2
Evap Energy Density = 10kW/m2
Evap Energy Density = 12.5kW/m2

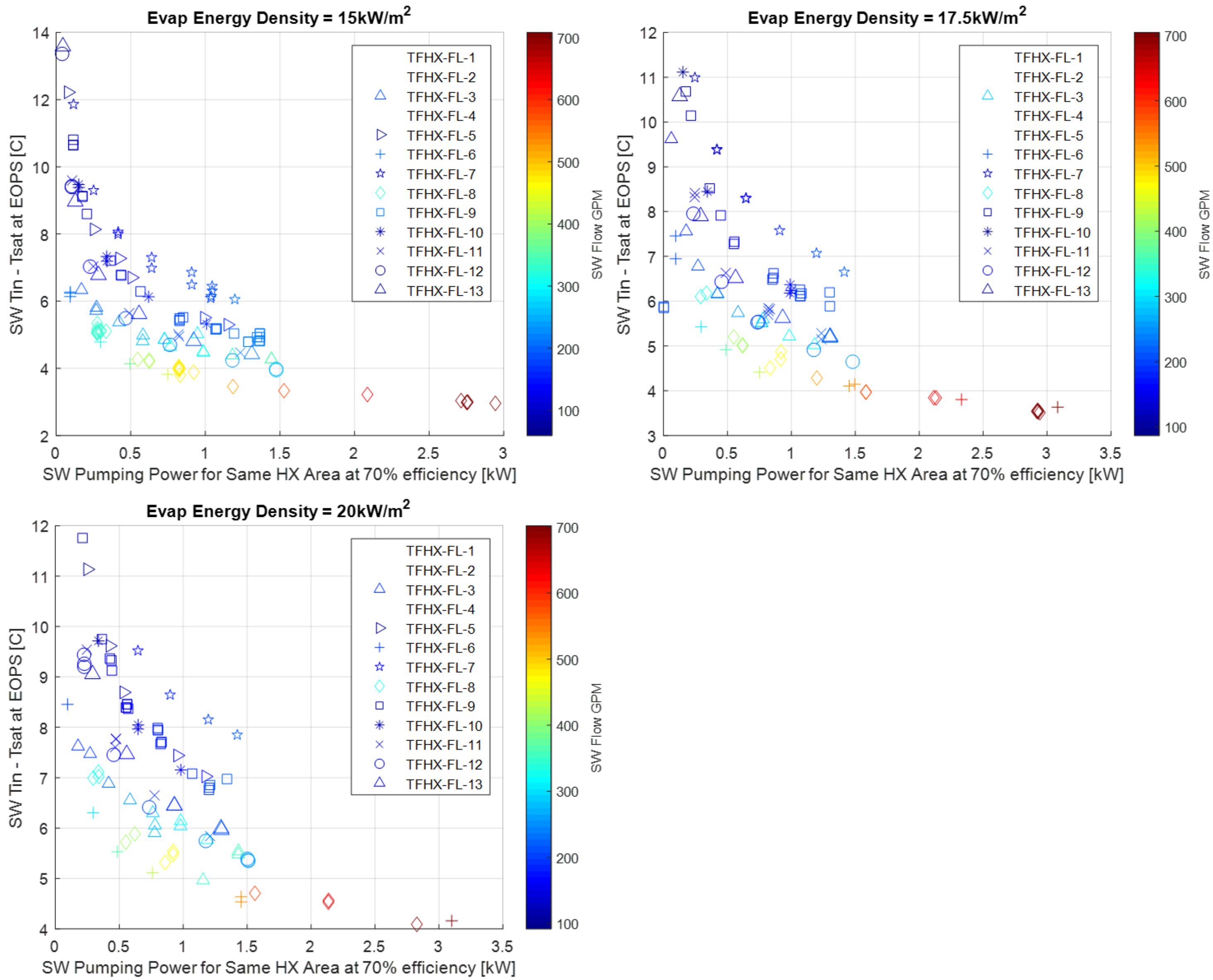

Figure 13. Evaporator approach temperature vs pumping power at different energy densities.

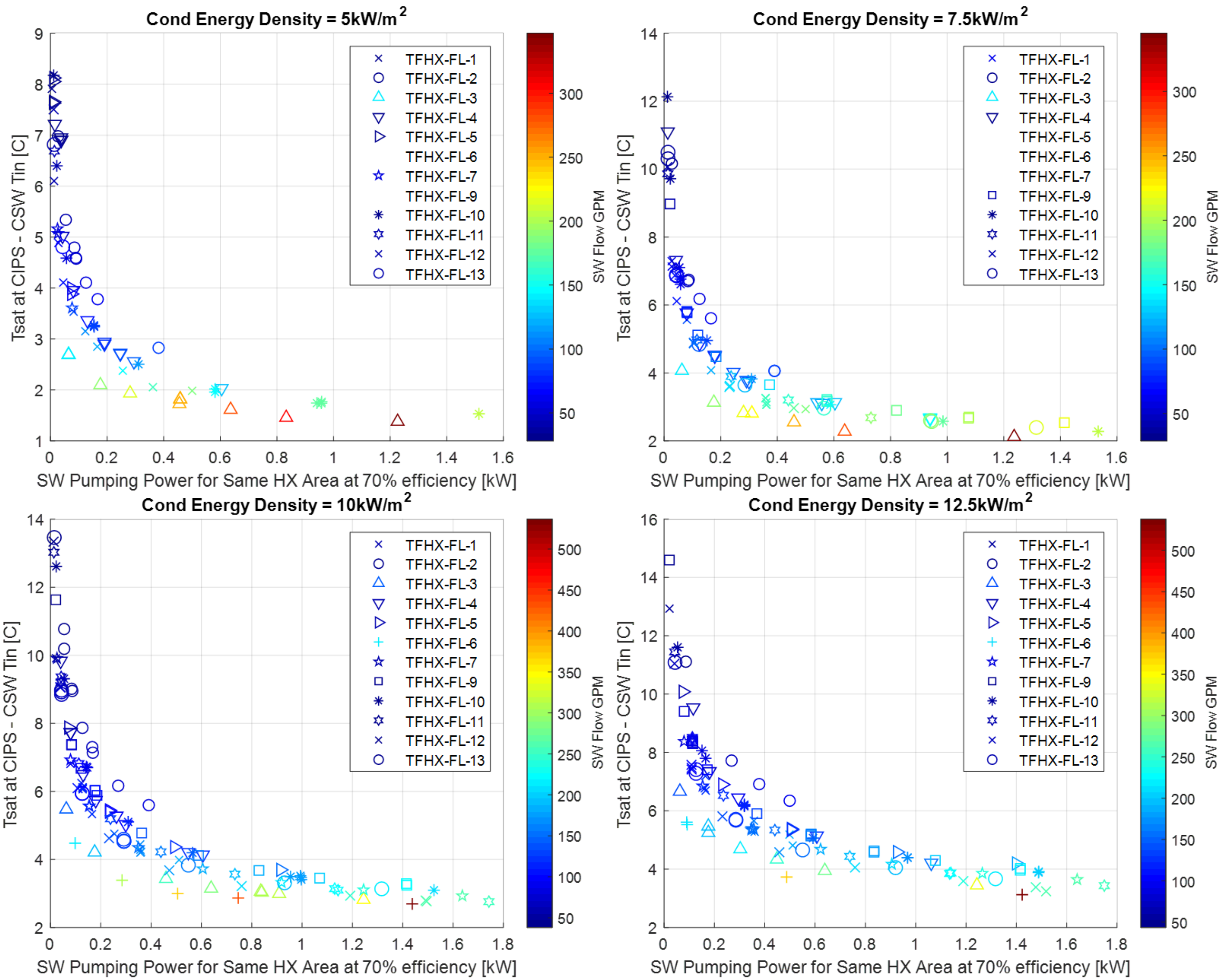

Cond Energy Density = 5kW/m^2
Cond Energy Density = 7.5kW/m^2
Cond Energy Density = 10kW/m^2
Cond Energy Density = 12.5kW/m^2
Tsat at CIPS - CSW Tin [C]
SW Pumping Power for Same HX Area at 70% efficiency [kW]
SW Flow GPM
TFHX-FL-1
TFHX-FL-2
TFHX-FL-3
TFHX-FL-4
TFHX-FL-5
TFHX-FL-6
TFHX-FL-7
TFHX-FL-9
TFHX-FL-10
TFHX-FL-11
TFHX-FL-12
TFHX-FL-13

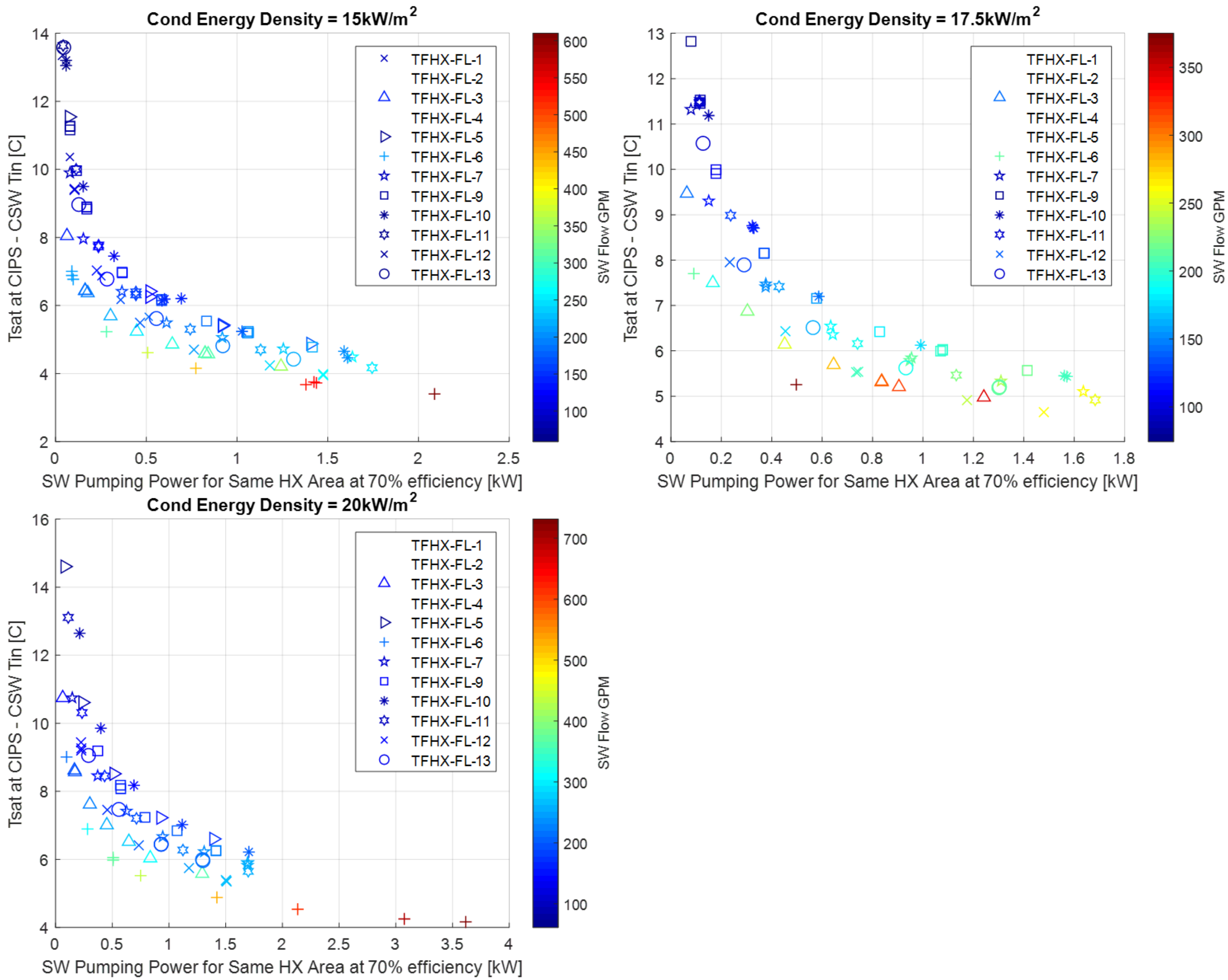

Figure 14. Condenser approach temperature vs pumping power at different energy densities.

4.3. DISCUSSION

4.3.1. Compactness

TFHXs contain more heat transfer area per cubic meter (m2/m3) than plate-and-frame, brazed fin, and shell-and-tube heat exchangers (Figure 15). FL-1 type (2.12-mm plate spacing units) and FL-3 type (4.24-mm plate spacing units) are in the same range of compactness compared to previous TFHX designs. At the same energy density, TFHXs require less than 25% of the volume of previously tested heat exchangers to produce the same duty (Figure 16).

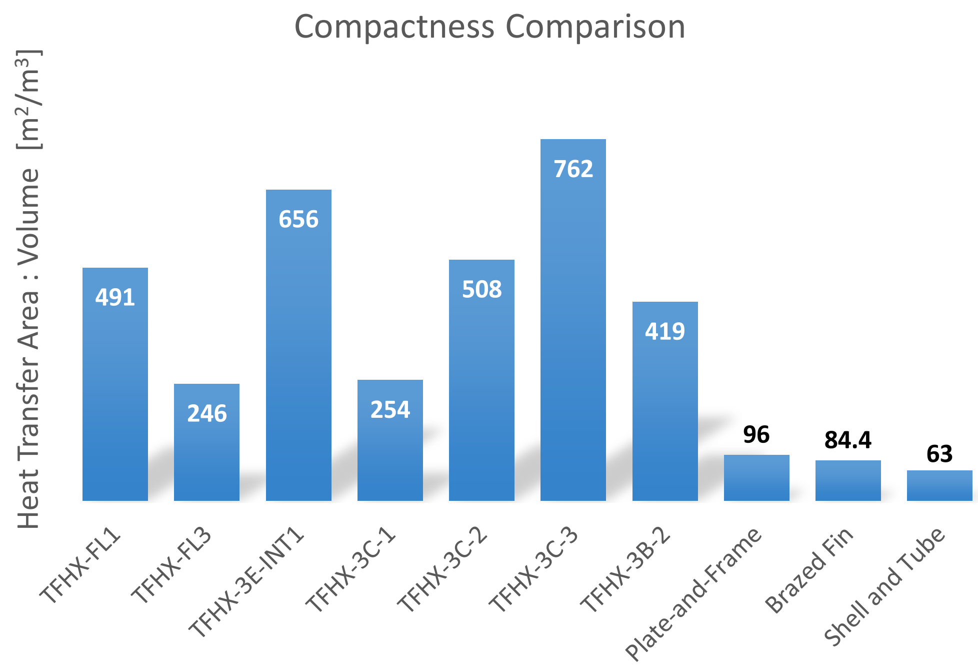

Figure 15. TFHX heat exchangers have more heat transfer area per volume compared to the previously tested plate-frame (APV), brazed fin (BAHX3), and shell and tube (ETHX) heat exchangers

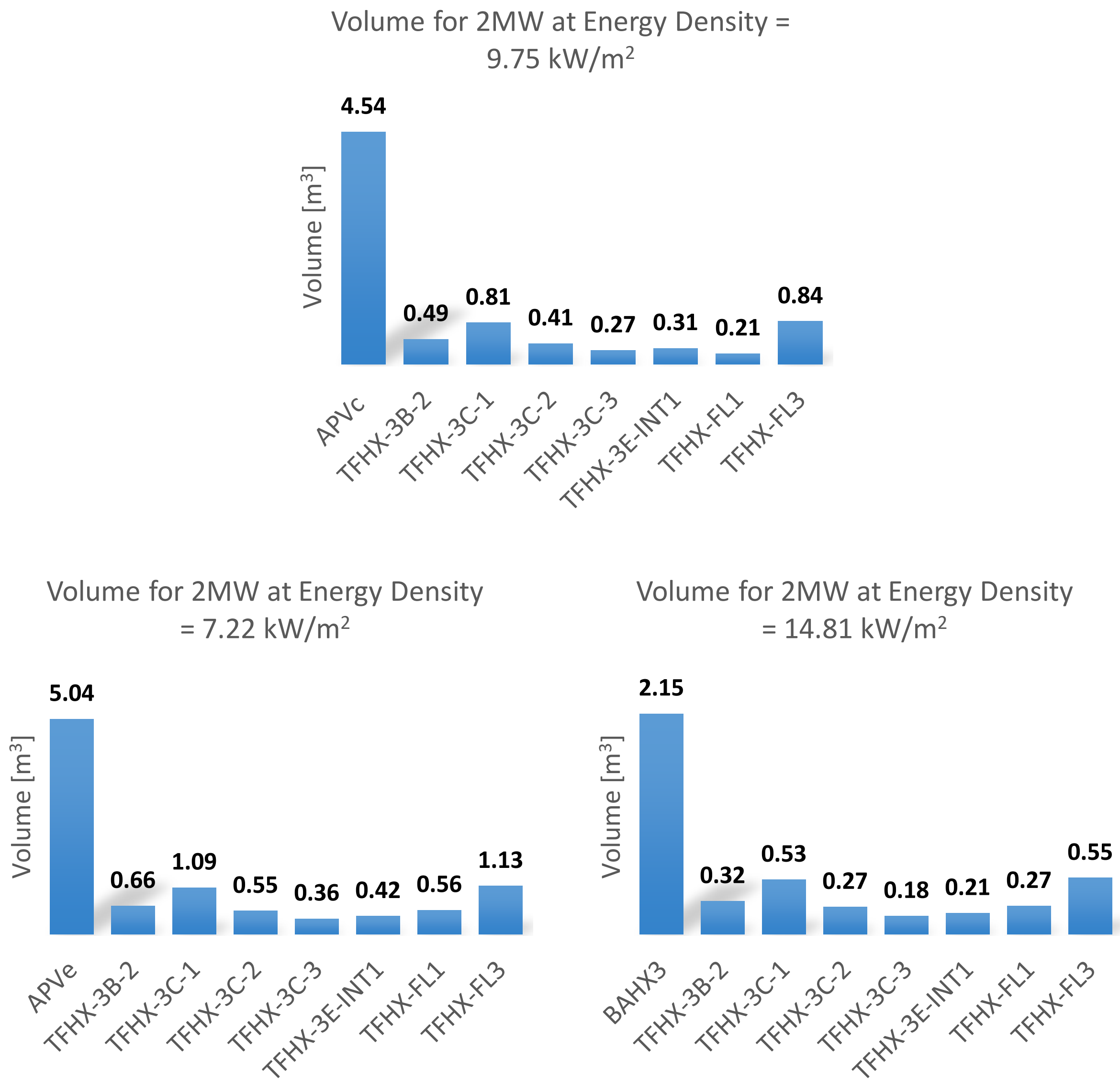

Figure 16. Comparison of volume required for 2MW of duty at various energy densities. Energy density was selected to match previously tested heat exchangers.

4.3.2. <u>OTEC Heat Exchanger Design</u>

Makai previously reported on the development of the OTEC Power Calculator, a tool to evaluate different heat exchanger designs in the context of an OTEC system performance. Heat exchangers can be compared in terms of area (i.e., heat exchanger cost) or volume (i.e., system size and cost) required to produce a targeted net power. The calculator takes into account seawater flow rates through the heat exchangers *and* the system (cold water pipe, intake screen, discharge pipe).

The best heat exchanger design was established by setting the heat exchanger area and seawater temperature and varying seawater flow rates and turbine parameters to maximize net power. Previous results had FL-1 and FL-5 as the best performing evaporator and condenser, respectively.

However, the optimal operating point was just outside the tested data range for FL-1, which led to some uncertainty in the results.

In this period, the same analysis was applied to the new heat exchanger designs. For evaporators, FL-12 produced 3.4% less net power compared to FL-1 (Figure 17). If the original FL-1 predicted result was off by 5 kPa due to extrapolation errors, then FL-12 and FL-1 have comparable net power production.

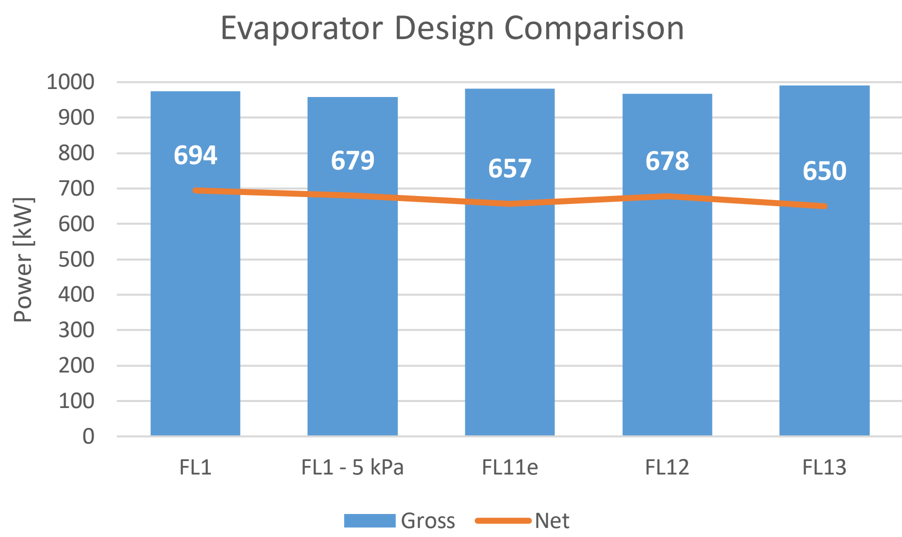

Figure 17. Comparison of evaporator designs in OTEC system.

For condensers, FL-5 is still the overall best design (Figure 18). FL-13 is the next best design.

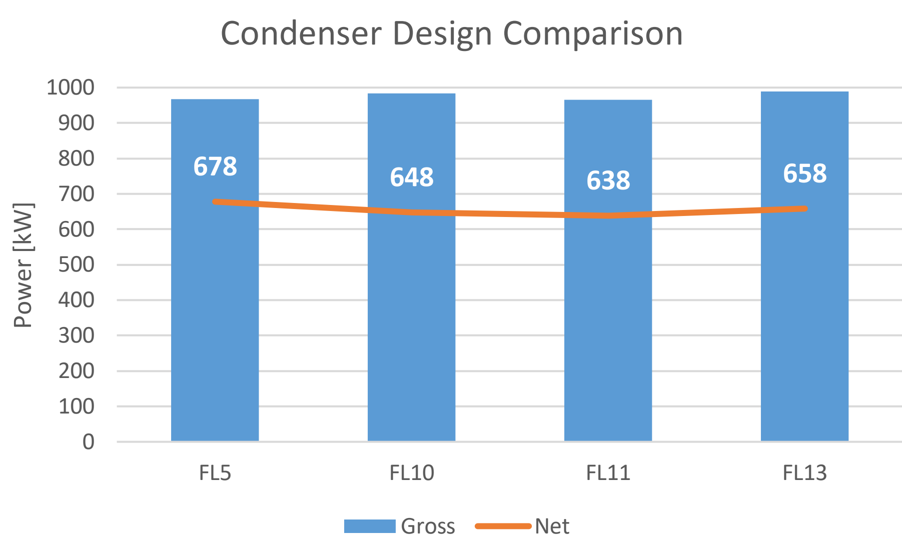

Figure 18. Comparison of condenser designs in OTEC system.

5. TFHX CHARACTERIZATION

In this period, Makai focused on investigating fatigue life and establishing an S-N curve for a single pattern design. Makai also evaluated the consistency of the internal channel size across a small plate and between plates of the same design.

5.1. CYCLIC PRESSURE TESTING

Makai designed and carried out a fatigue test plan to understand how plate design parameters and operating conditions (mean and alternating pressure) affected fatigue life. Makai began our fatigue testing program by testing individual plates of different designs but quickly realized it is impractical to test every configuration. Instead, we focused the fatigue testing program on understanding trends in how fatigue life is affected by changes in design parameters. This information is used to guide initial plate design. The final plate is then tested under the expected operating conditions for empirical fatigue life data and, if necessary, modifications to the design are made to improve fatigue life.

In early testing, many samples failed at transition zone welds or the seal weld. In subsequent plate designs, the goal was to strengthen the transition zone welds such that failures would occur in the pattern zone. This way, the limits of the main heat transfer region, which is it key to the TFHX technology would be tested. An actual plate may have a lower fatigue life if the transition zone welds had to be re-designed, e.g., to allow for larger flow channels; the fatigue life will be determined through testing of the final plate design.

In general, stronger plates (plates with higher supported burst pressures) had higher cycles to failure under the same alternating pressure cycling condition. Makai tested four variations on an additional fabrication step and found the cycles to failure increased by 3-7X but also changed the internal channel geometry. The most significant factor that affects fatigue life is the magnitude of alternating pressure. Lower alternating pressures correlated with increased cycles to failure. Lower ratios of alternating pressure to supported burst pressure also correlated with increased cycles to failure. The mean pressure had no significant effect on fatigue life.

Previous Fatigue Testing Data

Makai previously performed a series of fatigue testing but results were sometimes skewed by fixture bias and failures at non-pattern weld locations. For a test plate, failures at non-pattern weld locations are not necessarily indicative of actual plate performance because the transition weld and seal weld are likely different in the final plate design. When plates designed for an application are tested, failure locations are representative and the overall design must meet the application requirements, otherwise, re-design is necessary.

Full-length and cassette style plates were tested at representative OTEC/ammonia cyclic pressures. The 60-160 psig cycle represents a startup/shutdown cycle on the evaporator during testing at the OERC. During testing, the evaporator may see pressures up to 150 psig and when testing is over, the ammonia system is typically maintained at 60 psig (by running cold seawater through the condenser). Additionally, depending on the daily test points (duty and seawater flow rates), it is possible for both condenser and evaporator to experience pressure cycling within the 60-150 psig range up to 12 times in a day. These cycling conditions are only applicable during performance testing; in expected steady-state OTEC operations, pressure fluctuations are expected to be less than 5 psig.

Combined Data

The alternating pressure amplitude is the most significant factor in determining fatigue life. Using the ratio of alternating pressure to supported burst pressures is one way to view results for different pattern weld designs on the same plot (Figure 19 and Figure 20). The cycles to failure is roughly inversely proportional to the cube of the ratio of alternating pressure amplitude to the supported burst pressure. Trends for 0.003" and 0.004" samples are less clear because most of the failures occurred at transition welds or seal welds. In the 0.005" samples that failed at pattern welds, the cycles to failure are proportional to $\frac{1}{{\mathit{alternating\ pressure}/_{\mathit{supported\ burst\ pressure}}}^{3.4}}$. With variations on the additional fabrication step to extend fatigue life, the failure weld shifted to seal or transition welds and there was not enough data for a correlation. A correlation may not be useful because seal and transition weld designs are specific to an application.

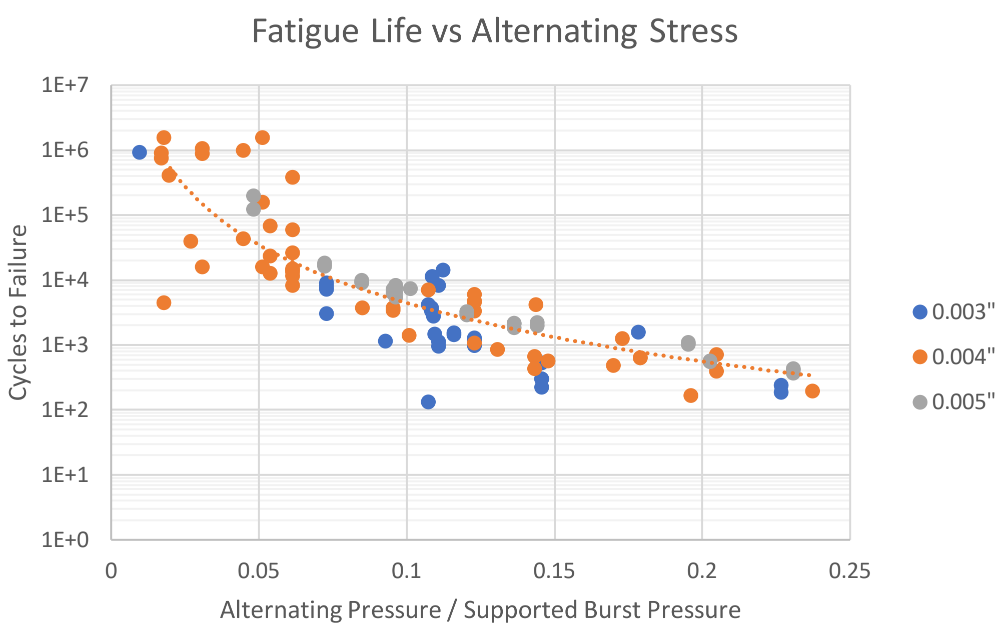

Figure 19. Cycles to failure vs ratio of alternating pressure amplitude/supported burst pressure. Data from 0.003" and 0.004" samples are from different plate shapes and mostly transition / seal weld failures. 0.005" data shows pattern failures only.

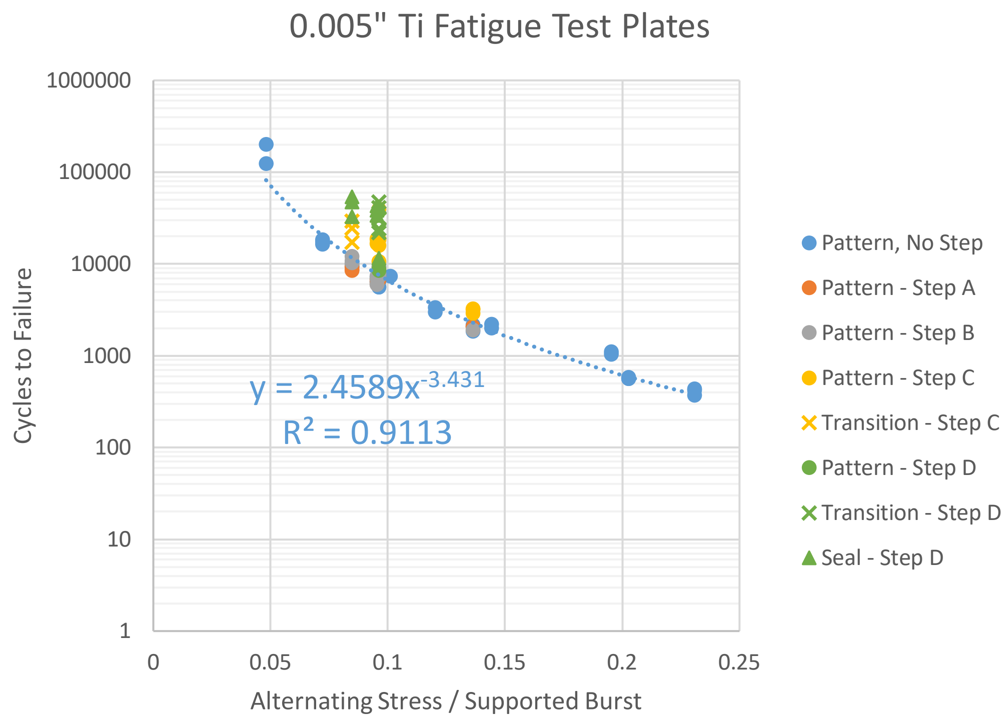

Figure 20. Effect of variation on additional fabrication step and alternating pressure on failure weld and cycles to failure.

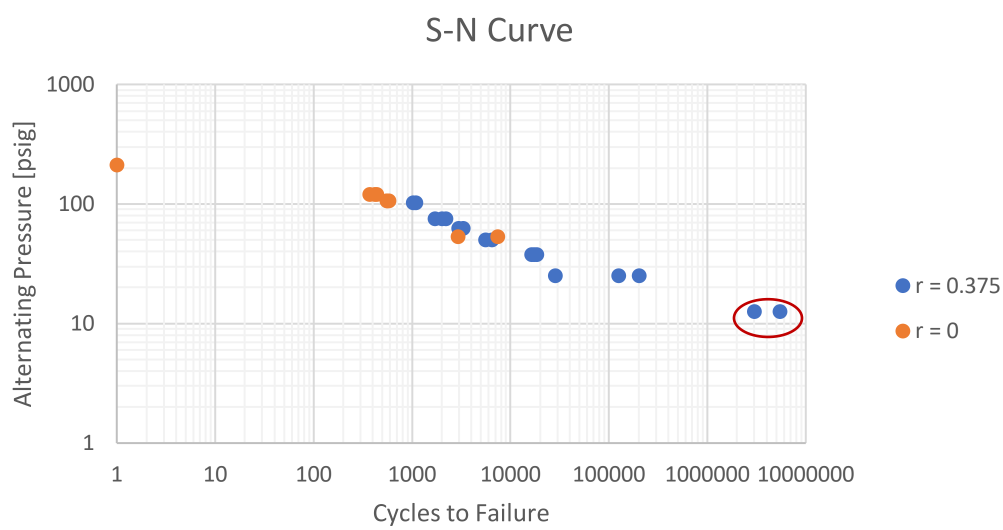

Figure 21. S-N Curve for 0.005” sample at two different stress conditions, r = 0 and r = 0.375.

5.1.1. Discussion

Designs that resulted in higher supported and unsupported burst pressures also had increased cycles to failure under the same pressure cycling conditions.

For the same plate design, adding a step to the fabrication process had the potential to increase cycles to failure up to 8X and shift the failure location also changed from pattern welds to either seal or transition welds.

Cycles to failure is strongly dependent on the alternating pressure amplitude. High alternating pressures have shorter cycles to failure. For the two cases tested ($r = 0$ and $r = 0.375$), the reversible stress condition did not have significant impact on cycles to failure (Figure 21).

Plate designs must still be evaluated for each specific application. The expected pressure cycles, operating pressure, overall plate shape, effective channel size, and required lifetime will drive the design. At a minimum, fatigue testing should be performed at startup/shutdown pressure cycles and at operating pressure cycles to verify the plate design. Key things to look at for include unintentional stress concentration sites due to the overall plate shape and transition zone designs that are matched to the pattern weld strength or sufficient for the application.

5.2. INTERNAL CHANNEL CONSISTENCY

Heat exchanger performance assumes duty is distributed evenly from plate to plate. Significant deviations in internal channel size will affect the flow distribution of both internal and external fluids and cause uneven duty distribution between plates.

Makai constructed 10 small (80mm x 100mm) plates out of 0.006” Haynes 230 foil. Expansion pressures ranged from 6,000 to 6,300 psi. The effective internal channel size was measured in at least 9 locations on each of the 10 plates (Figure 22). Additionally, 5 line scans per plates were performed on 2 plates to evaluate the consistency of the shape of the internal channel (Figure 23).

In general, the internal channel sizes were consistent. The difference between the largest and smallest individual measurement was 0.07 mm. The difference in plate-to-plate average internal channel sizes was 0.01 mm (~2.5%) which is unlikely to significantly impact heat transfer distribution between plates.

In the overlay of line scans, the range between the maximum peak heights was 0.10 mm. The line scans are less precise because any background slope due to a slant in the plate must be manually subtracted. Also, depending on the geometry of the internal channel, profilometer measurements could not be obtained over certain areas due to the reflection off the surface.

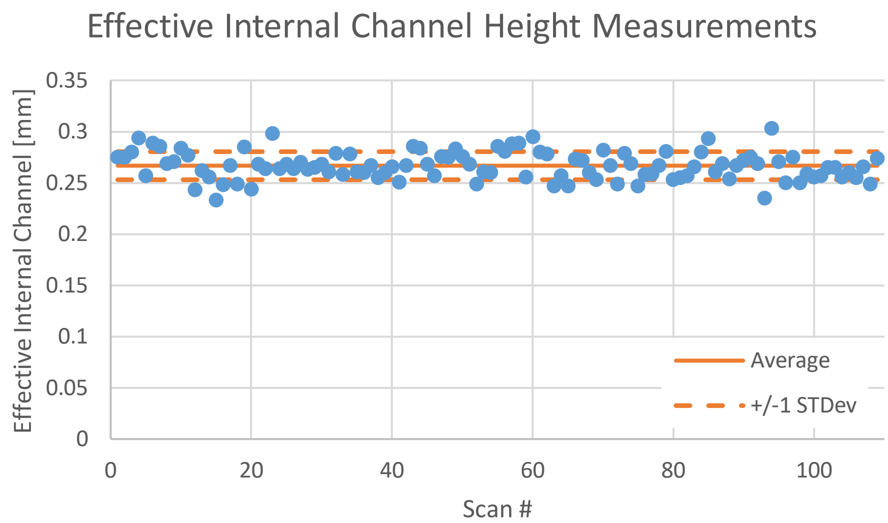

Figure 22. Effective internal channel size measurements on 10 plates.

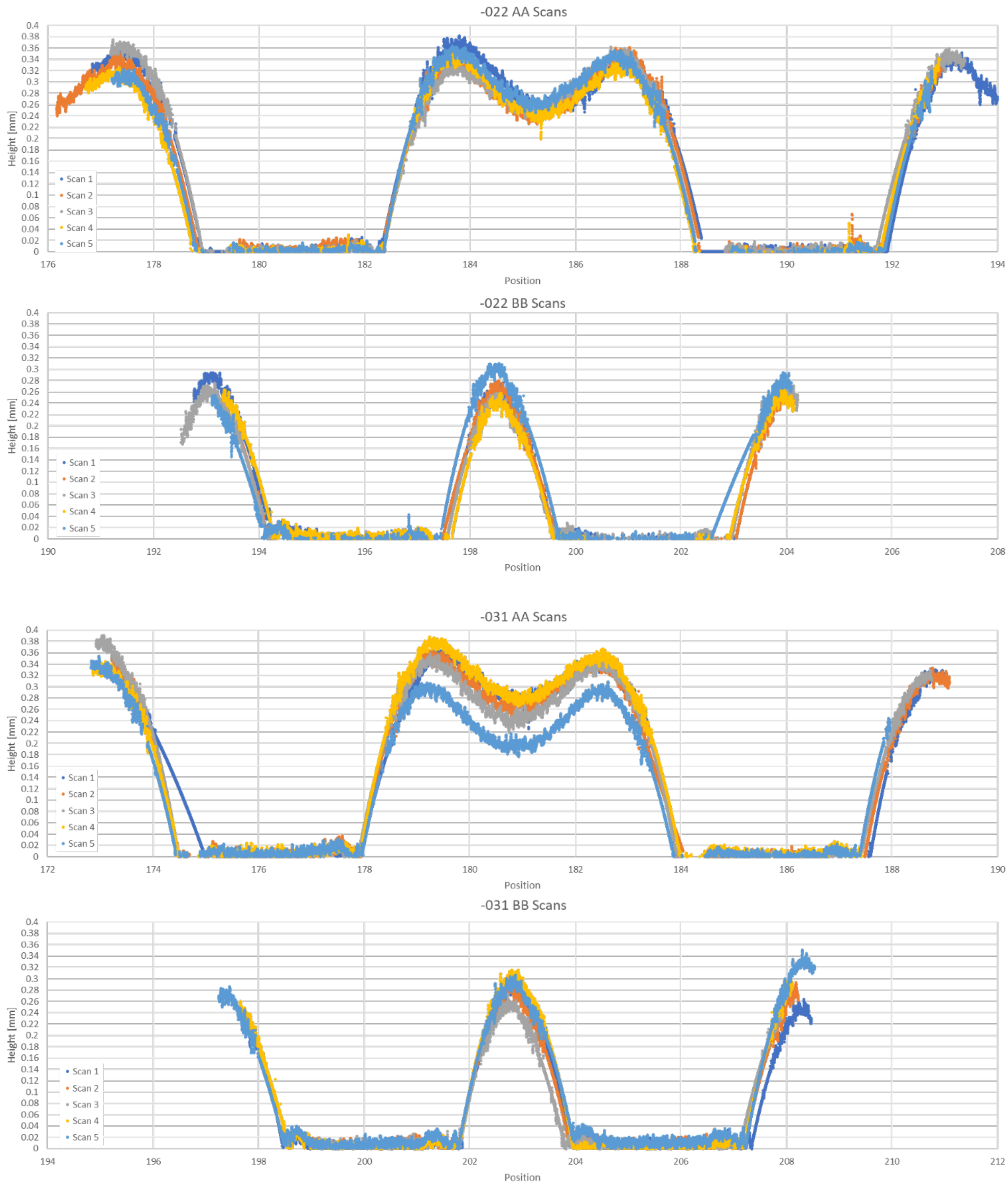

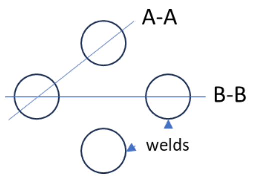

Figure 23. Overlay of line scans on two plates. 10 scans were performed on each plate; 5 scans across the A-A profile and 5 scans across the B-B profile.

6. BIOFOULING

Untreated, biofouling can have a detrimental impact on heat exchanger performance by increasing the pressure drop through the heat exchanger and decreasing the heat transfer performance. Makai previously evaluated a commercially available biofouling mitigation device called the Zeta Rod and found it delayed the onset of biofouling by 30 days but eventually performance loss was comparable to the baseline (no mitigation) case. Makai prototyped an automated in-situ cleaning method. Makai also started a baseline (no mitigation) test of a TFHX unit with larger seawater channels.

7. SUMMARY

Between June 2023 – January 2024, Makai improved TFHX plate fabrication speed and success rate; constructed and performance tested additional full-length TFHX units; designed a cassette-style form factor for large-scale TFHXs; and prototyped new biofouling mitigation methods.

TFHX Design and Characterization. Makai finalized the pass-thru seawater air conditioning (TFAC) design and developed a cassette-style design for large-scale applications. A TFAC unit was delivered to Blue Ocean Mariculture as a case study. Testing of the cassette-style design is planned in 2024 under separately funded work.

In cyclic pressure testing, Makai found adding an additional fabrication step can lead to 3-8X increase in cycles prior to failure and shift failures from pattern welds to seal or transition welds. Lower ratios of alternating stress to supported burst pressure lead to longer cycles to failure.

Makai also performed multiple measurements on 10 prototype-scale plates and found the shape and size of the internal channel was consistent and the measured deviations were unlikely to cause uneven heat transfer distribution between plates.

TFHX Fabrication. Makai improved fabrication speed, implemented a new method to repair plates, and improved the quality of the cut-edge.

Plate fabrication time has improved 25%. During first two days of a production run, plate success rate was 78.5% but averaged across four days, the success rate decreased 10%. Makai continues to investigate the inconsistency between the first two days' and last two days' success rates. The new repair method contributed ~20% of the successful plates.

Finally, Makai improved the quality of the cut-edge with new fixturing. The remaining rough sections will be improved with software modification.

TFHX Performance Testing. In this period, Makai tested three ammonia-seawater (OTEC) four-port TFHXs. Performance data is fed into the OTEC Power Calculator to evaluate the different TFHX designs in the context of an OTEC power plant. The OTEC Power Calculator accounts for parasitic losses related to the total amount of seawater flow through the system, not just through the heat exchangers.

For a condenser, TFHX designs with larger plate spacings that optimize at higher volumetric flow rates are penalized because of the parasitic losses in the cold water pipe. For an evaporator, larger plate spacings that require higher volumetric flow rates are penalized because the intake screen must be larger to limit the approach velocity. Larger plate spacings also increase the overall OTEC system volume, which leads to larger (and more expensive) support structures. However, there is also the issue of biofouling mitigation to consider when selecting the evaporator design. Larger plate spacings may be easier to clean and ultimately lead to higher performance because the heat transfer surfaces won't be fouled.

TFHX designs tested in this period were compared to previous designs in the OTEC Power Calculator. The best designs remain TFHX-FL1 and TFHX-FL5 for the evaporator and condenser, respectively. However, the optimized operating point was outside the tested range for TFHX-FL1 and, therefore, Makai has selected TFHX-FL12 as the new evaporator design. TFHX-FL12 is predicted to produce 3.5% less net power compared to TFHX-FL1, but the operating point was within the tested data range, providing more confidence in the prediction.

Biofouling. Makai designed, built, and tested a prototype for automated in-situ cleaning and started a baseline (no biofouling mitigation) test. In both units, there was no change in pressure drop vs flow after 30 days (as expected). Testing will continue for at least 90 days; in previous tests, performance degradation was observed within 90 days.

Upcoming Work

The major points of focus for Makai's near-term work are to:

- Identify factors in fabrication environment and/or procedure that lead to inconsistencies in plate success rates
- Improve cut edge quality
- Continue SW-NH3 performance testing to identify optimal OTEC design, and
- Continue to develop, prototype and test in-situ biofouling control/mitigation systems
-